Article:

Reinhard, AA, Jackson, MG, Harvey, J et al. (2 more authors) (2016) Extreme differences in 87Sr/86Sr between Samoan lavas and the magmatic olivines they host: Evidence for highly heterogeneous 87Sr/86Sr in the magmatic plumbing system sourcing a single lava. Chemical Geology, 439. pp. 120-131. ISSN 0009-2541

https://doi.org/10.1016/j.chemgeo.2016.05.017

Extreme differences in $^{87}Sr/^{86}Sr$ between Samoan lavas and the magmatic olivines they host: Evidence for highly heterogeneous $^{87}Sr/^{86}Sr$ in the magmatic plumbing system sourcing a single lava.

A.A. Reinhard[1], M.G. Jackson[1], J. Harvey[2], C. Brown[3], J.M. Koornneef [4]

[1] University of Calfornia Santa Barbara, Department of Earth Science, Santa Barbara, CA, 93109-9630, USA (reinhard@umail.ucsb.edu)

[2] University of Leeds, School of Earth and Environment, Leeds, UK

[3] Stony Brook University, Department of Geosciences, Stony Brook, NY

[4] Vrije Universiteit Amsterdam, Faculty of Earth and Life Sciences, Amsterdam, NL.

ABSTRACT

Investigations of mantle heterogeneity in ocean island basalts (OIB) frequently compare heavy radiogenic isotopes (i.e. $^{87}Sr/^{86}Sr$), often measured in whole rock powders, with $^{3}He/^{4}He$ and $\delta^{18}O$, commonly measured in olivines. However, the $^{87}Sr/^{86}Sr$ in the olivines, which is dominated by Sr in melt inclusions, may not be in equilibrium with the $^{87}Sr/^{86}Sr$ in the whole rock. Here we present new $^{87}Sr/^{86}Sr$ measurements made on Samoan magmatic olivines, where multiple olivine crystals are aggregated for a single isotopic measurement. The olivines host abundant melt inclusions, and yielded relatively large quantities of Sr (13.0 to 100.6 ng) in 19 to 185 mg aliquots of fresh olivine, yielding high Sr_{sample}/Sr_{blank} ratios ($\geq$ 427). These new data on olivines show that samples can exhibit significant $^{87}Sr/^{86}Sr$ disequilibrium: in one extreme sample, where the basaltic whole rock $^{87}Sr/^{86}Sr$ (0.708901) is higher than several different aliquots of aggregate magmatic olivines (0.707385 to 0.707773), the whole rock-olivine $^{87}Sr/^{86}Sr$ disequilibrium is >1590 ppm. The $^{87}Sr/^{86}Sr$ disequilibrium observed between whole rocks and bulk olivines relates to the isotopic disequilibrium between whole rocks and the average $^{87}Sr/^{86}Sr$ of the population of melt inclusions hosted in the olivines. Therefore, a population of olivines in a Samoan lava must have crystallized from (and trapped melts of) a different $^{87}Sr/^{86}Sr$ composition than the final erupted lava hosting the olivines. A primary question is how melts with different $^{87}Sr/^{86}Sr$ can

exist in the same magmatic plumbing system and contribute heterogeneous $^{87}Sr/^{86}Sr$ to a lava and the magmatic olivines it hosts. We explore potential mechanisms for generating heterogeneous melts in magma chambers. The reliance, in part, of chemical geodynamic models of the relationships between isotopic systems measured in whole rocks ($^{87}Sr/^{86}Sr$) and systems measured in olivines ($^{3}He/^{4}He$ and $\delta^{18}O$) means that whole rock-olivine Sr-isotopic disequilibrium will be important for evaluating relationship among these key isotopic tracer systems. Moving forward, it will be important to evaluate whether whole rock-olivine Sr-isotopic disequilibrium is a pervasive issue in OIB globally.

Keywords: Melt inclusions, Samoa, hotspot, $^{87}Sr/^{86}Sr$, $^{3}He/^{4}He$, $\delta^{18}O$, Mantle Geochemistry

1. INTRODUCTION

The composition of the Earth's mantle, as sampled by ocean island basalts (OIB) erupted at intraplate volcanic hotspots, is highly heterogeneous (Gast et al., 1964; White, 1985, 2015; Zindler and Hart, 1986; Hofmann, 1997). The origin of the heterogeneity in the mantle has been attributed to subduction of oceanic and continental crust (and associated sediments) into the mantle over geologic time (White and Hofmann, 1982; Hofmann and White, 1982). The geochemical diversity of the mantle has been subdivided into several broad endmember compositions including depleted mantle (DM) compositions (characterized by unradiogenic Sr and Pb isotopic compositions and radiogenic $^{143}Nd/^{144}Nd$), HIMU ("high μ", or $^{238}U/^{204}Pb$, characterized by highly radiogenic Pb isotopic compositions), EM1 (or enriched mantle I, characterized by unradiogenic Pb and geochemically enriched $^{87}Sr/^{86}Sr$ and $^{143}Nd/^{144}Nd$) and EM2 (enriched mantle II, characterized by intermediate Pb isotopic compositions and geochemically enriched $^{87}Sr/^{86}Sr$ and $^{143}Nd/^{144}Nd$). However, the distribution and lengthscales of geochemical heterogeneity in the mantle, as sampled by oceanic basalts, are still poorly constrained.

Lavas from the Samoan hotspot—an age-progressive volcanic chain (Hart et al., 2000; Staudigel et al., 2006; Sims et al., 2008; Koppers et al., 2008, 2011) located in the southwest Pacific—exhibit a remarkable range of geochemical compositions, including the most geochemically enriched EM2 signatures globally (Fig. 1; supplementary Table 1). Lavas dredged from the deep submarine flanks of Savai'i Island, the westernmost island in Samoa, have whole rock $^{87}Sr/^{86}Sr$ ratios that extend up to 0.720469 (Jackson et al., 2007a). This represents the highest $^{87}Sr/^{86}Sr$ observed in a lava erupted in the world's ocean basins (Fig. 1). This geochemically enriched $^{87}Sr/^{86}Sr$ is characteristic of the EM2 signature and is the result of recycled ancient terrigenous sediment sampled by the Samoan plume (Jackson et al., 2007a; Workman et al., 2008). However, Samoan lavas can host $^{87}Sr/^{86}Sr$ ratios as low as 0.7044, and a subset of these lavas exhibit primitive, high $^{3}He/^{4}He$ ratios (Farley et al., 1992; Workman et al., 2004; Jackson et al., 2007, 2010, 2014). For example, lavas from the Samoan island of Ofu exhibit $^{3}He/^{4}He$ ratios up to 33.8 Ra (ratio to atmosphere), consistent with elevated $^{3}He/^{4}He$ identified in Samoan lavas from earlier studies (Farley et al., 1992; Workman et al., 2004, Jackson et al., 2007b).

Radiogenic isotopic analysis of whole rock lavas can obscure the geochemical diversity that may exist within in a single lava. For example, individual olivine-hosted melt inclusions from Samoan basalts can have dramatically different $^{87}Sr/^{86}Sr$ than the host whole rock, which provides an important clue that magmatic olivines can trap melts of diverse mantle sources (Jackson and Hart, 2006). Jackson and Hart (2006) were the first to measure Sr isotopes in individual olivine-hosted melt inclusions, and they targeted Samoan lavas in their study. Using laser ablation multi collector inductively coupled plasma mass spectrometry (LA-MC-ICP-MS), they found that the $^{87}Sr/^{86}Sr$ ratios in melt inclusions recovered from a single Samoan basalt can vary by up to 0.34% (3,400 ppm), and the $^{87}Sr/^{86}Sr$ variability in Samoan melt inclusions greatly exceeds the external precision (±320 ppm, 2σ) of the melt inclusion measurements. The observation that olivine-hosted melt inclusions in OIB can host different ^{87}Sr/^{86}Sr than the whole rock was supported by later work: Harlou et al. (2009) micro-milled olivine-hosted melt inclusions from Icelandic basalts, and Sr was separated from the milled inclusion powders by standard column chemistry and analyzed by thermal ionization mass spectrometry (TIMS). Their results also show that ^{87}Sr/^{86}Sr in olivine-hosted melt inclusions can be significantly different from the whole rock (by >6000 ppm). In a recent LA-ICP-MS study focusing on Hawaiian lavas, Sobolev et al. (2011) further demonstrated that the ^{87}Sr/^{86}Sr of olivine hosted melt inclusions can vary dramatically (from 0.7021 to 0.7081) within a single lava. In summary, ^{87}Sr/^{86}Sr measured in olivine-hosted melt inclusions reveal that isotopically heterogeneous components exist in OIB that are not observed in whole rock analyses.

In a parallel effort to evaluate the presence of extreme ^{87}Sr/^{86}Sr heterogeneity within the different components hosted in a single Samoan lava, Jackson et al. (2009) targeted fresh magmatic clinopyroxenes (cpx) separated from lavas that were shown by Jackson and Hart (2006) to have heterogeneous ^{87}Sr/^{86}Sr in olivine-hosted melt inclusions. Two of the samples (AVON3-78-1 and AVON3-71-2), that exhibit extreme ^{87}Sr/^{86}Sr variability in olivine-hosted melt inclusions (Jackson and Hart, 2006), had two populations of visually-distinct cpx (green and black) separated and analyzed for ^{87}Sr/^{86}Sr. Similar to the ^{87}Sr/^{86}Sr of the melt inclusion populations from these lavas, the ^{87}Sr/^{86}Sr from each cpx population is lower than the respective whole rock lava (by as much as ~1700 ppm for AVON3-78-1 and ~650 ppm for AVON3-71-2). The lavas with the most extreme cpx-whole rock Sr-isotopic disequilibrium and the greatest diversity in melt inclusion compositions (AVON3-78-1 and AVON3-71-2) are extremely fresh (Workman et al., 2004) and effectively zero-age (<8 Ka; Sims et al., 2008), and thus the ^{87}Sr/^{86}Sr heterogeneity within these basalts cannot be due to alteration or post-eruptive radiogenic ingrowth. Jackson et al. (2009) concluded that geochemically-diverse magmas with different $^{87}Sr/^{86}Sr$ mix at depth, thereby generating the Sr-isotopic disequilibrium observed in the different components of the lava, including olivine-hosted melt inclusions and cpx.

This study targets aggregated magmatic olivines for $^{87}Sr/^{86}Sr$ measurement (i.e., multiple olivine crystals are pooled for a single $^{87}Sr/^{86}Sr$ analysis). Strontium is highly incompatible in the olivine lattice (olivine-basaltic melt partition coefficients for Sr are ~10^{-4}; Beattie, 1994), thus nearly all Sr in olivine is hosted in melt inclusions. Therefore, measurement of $^{87}Sr/^{86}Sr$ in magmatic olivines provides an average $^{87}Sr/^{86}Sr$ for the melt inclusion population hosted in olivines. The pooling of many olivines for a single $^{87}Sr/^{86}Sr$ analysis is advantageous because it generates larger quantities (up to ~100 ng of Sr in 185 mg of magmatic olivines, see Data section below) of Sr for analysis, thereby overcoming the technical challenges associated with accurate and precise measurement of $^{87}Sr/^{86}Sr$ in a single inclusion (Jackson and Hart, 2006; Harlou et al., 2009; Sobolev et al., 2011). One disadvantage to this approach is that pooling hundreds of olivines for a single $^{87}Sr/^{86}Sr$ analysis can “mask” the full variability in the melt inclusion population (Ramos and Reid, 2005; Harlou et al., 2009). Nonetheless, if analysis of aggregated olivines are shown to have different $^{87}Sr/^{86}Sr$ than the host whole rock, it would provide independent confirmation of the result of the Jackson and Hart (2006) LA-ICP-MS study showing that olivine-hosted melt inclusions have different $^{87}Sr/^{86}Sr$ than the whole rock.

Here we report extreme $^{87}Sr/^{86}Sr$ disequilibrium between Samoan basalts and the olivines they host. The discovery of Sr-isotopic disequilibrium between whole rocks and olivines has important implications for magmatic processes operating at depth and impacts the possible interpretations of the relationships between $^{87}Sr/^{86}Sr$ (which is frequently measured in the whole rock) and $^{3}He/^{4}He$ and $\delta^{18}O$ (which are frequently measured in olivines). Critically, the discovery that olivine $^{87}Sr/^{86}Sr$ can be significantly different from whole rock $^{87}Sr/^{86}Sr$ indicates that established relationships between $^{3}He/^{4}He$ and $^{87}Sr/^{86}Sr$ will be modified if $^{3}He/^{4}He$ and $^{87}Sr/^{86}Sr$ are both measured in olivines. This is fundamentally important for chemical geodynamics, which seeks to explain how relationships between various isotopic systems—including $^{87}Sr/^{86}Sr$ and $^{3}He/^{4}He$—evolved in Earth's dynamic mantle.

2. METHODS

This study focuses on olivine samples from 10 young (<1 Ma; Sims et al., 2008; McDougall, 2010; Koppers et al., 2011) and fresh (Workman et al., 2004; Jackson et al., 2010; Hart and Jackson, 2014) lavas from the Samoan hotspot track, which helps to minimize $^{87}Sr/^{86}Sr$ variability introduced by (1) post-eruptive radiogenic ingrowth of ^{87}Sr by decay of ^{87}Rb and (2) alteration of the lavas. The samples represent submarine and subaerial shield-stage lavas from 5 volcanoes (Ofu, Malumalu, Vailulu'u, Ta'u and Muli; Workman et al., 2004; Jackson et al., 2007b). The analytical campaign sought to characterize $^{87}Sr/^{86}Sr$ in aggregated olivine separates from geochemically well-characterized whole rock lavas. For analysis, up to 100 olivines hosting visible (under binocular microscope) melt inclusions from each basalt sample were aggregated, dissolved, and analyzed for $^{87}Sr/^{86}Sr$ by TIMS.

A subset of the lavas examined here were previously characterized for $^{3}He/^{4}He$ and $\partial^{18}O$ (both measured in olivines; Table 1), whole rock Sr, Nd, and Pb isotopic ratios, whole rock major and trace element concentrations, and volatile element concentrations measured on glasses (Workman et al., 2004; Jackson et al., 2007a, 2007b, 2010; Workman et al., 2006, 2008; Salters et al., 2011; Jackson and Shirey, 2011). The major element concentrations of a representative suite of olivines from each sample (not the olivines dissolved for analyses) were analyzed by electron microprobe. Whole rock major element concentrations were measured by XRF on whole rock powders prepared from two Samoan lavas, AVON3-63-11 and AVON3-63-2 (see supplementary Table 2). Then XRF analyses were carried out at Washington State University with the other Samoan "AVON3" samples published in Workman et al. (2004).

2.1. $^{87}Sr/^{86}Sr$ analysis in olivines by TIMS:

$^{87}Sr/^{86}Sr$ measurements were conducted at the Boston University TIMS facility. 69 to 185 mg of the freshest, most pristine olivines were separated from each whole rock sample and pooled for $^{87}Sr/^{86}Sr$ analysis. Two samples (AVON3-71-2 and AVON3-68-11) hosted two visually distinct olivine populations (green and brown; each with a distinct forsterite compositions; Fig. 2). For these two samples, an aliquot of each olivine population was analyzed for $^{87}Sr/^{86}Sr$. Thus, 12 aliquots of olivine separates from 10 basalt samples were analyzed for $^{87}Sr/^{86}Sr$ (Table 1).

The olivines were leached and sonicated in 25ºC 6N HCl to remove all adhering groundmass and surface alteration. Following leaching, the samples were cleaned by sonication in milli-Q water. The olivine samples were then inspected for remaining groundmass or adhering alteration phases using a binocular microscope. If no such material remained, the leached samples were then weighed and dissolved in concentrated HF and 6N nitric acid at 140 °C. (Note that the olivines were not powdered prior to dissolution, as powdering contributes additional Sr blank to the olivines.) An ^{84}Sr spike was then added to the solution and Sr was purified from the spiked Sr solution by column chemistry using Eichrom Sr spec resin (Harlou et al., 2009**)**. The Sr was then analyzed for $^{87}Sr/^{86}Sr$ and Sr concentrations by isotope dilution (ID) TIMS. Total procedural blanks (from sample dissolution to loading on the filament) for the $^{87}Sr/^{86}Sr$ analyses varied from 19 to 53 picograms of Sr, and blanks generally improved as the method was refined. Total procedural blanks were insignificant in comparison to the amounts of Sr measured in the bulk olivine separates: 14 to 101 nanograms of Sr were isolated from each batch of olivine separates, and Sr_{sample}/Sr_{blank} varied from 427 to 2905 during analysis of olivines.

All $^{87}Sr/^{86}Sr$ analyses in this study were conducted on a ThermoFinnigan Triton Thermal Ionization Mass Spectrometer (TIMS) outfitted with 10^{11} ohm amplifiers. A static multicollection routine with a standard cup configuration was used. All measured $^{87}Sr/^{86}Sr$ ratios were corrected for mass bias relative to $^{86}Sr/^{88}Sr$ of 0.1194 using an exponential law. During the course of this study, the Sr standard (NBS 987) was run during the same analytical sessions as the olivines. The filament loads of the standard runs bracket the range of Sr loads from the olivine separates: 100 nanograms (0.710249±0.000011, 2σ, n=8) and 4 nanograms (0.710249±0.000030, 2σ, n=8).

Following correction for spike addition and for mass bias, measured olivine sample $^{87}Sr/^{86}Sr$ ratios were then normalized to an $^{87}Sr/^{86}Sr$ of 0.710240 for SRM 987. A final blank correction was applied to all samples: due to the high sample-to-blank ratios, and the relatively consistent $^{87}Sr/^{86}Sr$ value of the blank (0.7099±0.0017, 2σ, n=6)--which is similar to the $^{87}Sr/^{86}Sr$ ratios in Samoan olivines--blank corrections to the $^{87}Sr/^{86}Sr$ ratio of the olivine separates were small (<16 ppm). The final corrected $^{87}Sr/^{86}Sr$ values of the olivines are reported in Table 1. The internal precision on the $^{87}Sr/^{86}Sr$ measurements of the olivine separates varied from 11 to 46 ppm (2σ), similar to the internal precision achieved on the NBS 987 standard runs. In order to evaluate the reproducibility of $^{87}Sr/^{86}Sr$ measurements on olivine unknowns, 4 different batches of visually-identical olivine separates from Samoan sample T25 were processed separately through all steps of chemistry and mass spectrometry over the course of 1 year, and the $^{87}Sr/^{86}Sr$ of the four analyses measured during two analytical sessions range from 0.704647 to 0.704662 (which represents 22 ppm total variation) (Table 1). The T25 olivines are homogeneous for $^{87}Sr/^{86}Sr$, and replicate analyses of these olivines shows that the method for measuring $^{87}Sr/^{86}Sr$ in olivine separates generates precise, reproducible data.

Additionally, a 77 mg aliquot of olivines from sample AVON3-78-1 was acid leached.

Following sample dissolution and Sr separation at the University of Leeds, the sample was analyzed using the ThermoFinnigan TIMS (using 10^{11} ohm amplifiers) hosted at the University of Leeds to provide an additional, replicate analysis in a different lab to evaluate the results presented in Table 1. A 5 ng aliquot of NBS987 run in the same analytical session as the olivine yielded a value of 0.710247±0.000012 (2σ), and employs the same mass bias correction reported above. The reported $^{87}Sr/^{86}Sr$ of the olivine analysis (Table 1) is corrected for the offset between this value and the preferred value (0.710240). The total procedural blank was 70 picograms, and the sample-to-blank ratio (547) results in a negligible blank correction to the final reported $^{87}Sr/^{86}Sr$ ratio. The $^{87}Sr/^{86}Sr$ of the replicate olivine analysis, obtained by ID-TIMS, yielded a value of 0.707773±0.000070 (2σ), which is 356 ppm higher than the $^{87}Sr/^{86}Sr$ analyses of a different batch of olivines from the sample basaltic sample made at Boston University.

A third $^{87}Sr/^{86}Sr$ measurement was made on AVON3-78-1 olivine using the ThermoFinnigan Triton-plus TIMS (using 10^{11} ohm amplifiers) at Vrije Universiteit (VU) Amsterdam (Koornneef et al., 2015). A separate 19 mg aliquot of olivines was prepared from AVON3-78-1 and acid leached. During the same analytical session, a 100 ng load of NBS 987 was analyzed and yielded an $^{87}Sr/^{86}Sr$ value of 0.710246±0.000005 (2σ), and follows the mass bias correction employed above. The $^{87}Sr/^{86}Sr$ of the olivine analysis is corrected for the offset between the measure and preferred (0.710240) NBS 987 ratio. The total procedural blank for this analysis was 28 pg, and the high sample to blank ratio (464) resulted in a negligible blank correction. The $^{87}Sr/^{86}Sr$ analysis and Sr concentration determination of the olivine was made by ID-TIMS; following blank correction and standard normalization, the $^{87}Sr/^{86}Sr$ is 0.707385±0.00009 (2σ), which is 192 ppm lower than the BU measurement and 547 ppm lower than the Leeds measurement.

All three $^{87}Sr/^{86}Sr$ measurements were made on aliquots of fresh olivines that were carefully leached prior to dissolution. Thus, it is unlikely that material adhering to the surface of the olivines (i.e., alteration phases, basaltic matrix, etc.) contributes to the $^{87}Sr/^{86}Sr$ variability observed in different aliquots of olivine from AVON3-78-1. Instead, the variability of $^{87}Sr/^{86}Sr$ between the three analyses is likely the result of sampling a heterogeneous olivine population: individual melt inclusions from sample AVON3-78-1 have highly variable $^{87}Sr/^{86}Sr$ (Jackson and Hart, 2006), and slightly different populations of olivines may have been analyzed during the Boston University, Leeds and the VU analyses. Nonetheless, the Leeds and VU $^{87}Sr/^{86}Sr$ analyses of AVON3-78-1 olivine are both lower (1591 and 2139 ppm respectively) than the whole rock, which confirms the result of significant olivine-whole rock Sr-isotopic disequilibrium. This contrasts with the four different aliquots of pristine olivine from Samoan sample T25, that give identical $^{87}Sr/^{86}Sr$ within measurement uncertainty (Table 1), which suggests a high degree of homogeneity in the melt inclusion population hosted in the olivines from this lava.

New $^{3}He/^{4}He$ measurements are not reported here; all $^{3}He/^{4}He$ measurements were obtained by crushing olivines in vacuo (see Kurz et al., 2004) and are reported in Workman et al. (2004) and Jackson et al. (2007b, 2010, 2014). It is possible to measure $^{87}Sr/^{86}Sr$ on olivine powder following crushing for helium isotopic measurement (thus permitting measurement of Sr and He isotopes on the same aliquot of olivines), but this procedure may result in a higher Sr blank contribution to the olivine powders following crushing. Careful measurements of Sr blank contributions from the crushing apparatus must be performed before $^{87}Sr/^{86}Sr$ and $^{3}He/^{4}He$ can be measured on a single olivine aliquot. Therefore, the $^{87}Sr/^{86}Sr$ measurements reported here were made on different aliquots of olivines than the $^{3}He/^{4}He$ measurements.

2.2. Major element analyses of olivines by electron probe.

Olivine major element analyses for 5 of the lavas examined here are reported in Jackson and Shirey (2011). Major element analyses for olivines from the remaining 5 lavas are reported here for the first time (supplementary Table 3). Representative olivine grains from each of these 5 lavas were separated. For two samples (AVON3-71-2 and AVON3-68-11), two visually-distinct olivine populations (green and brown) were identified in each lava, and representative olivines from each population were characterized. Therefore, in total, major element analyses of these 7 olivine populations from 5 different basalt samples (AVON3-68-11, AVON3-71-2, AVON3-73-2, ALIA104-04, Ofu 04-03) were completed on the Cameca SX-100 electron microprobe housed at UC Santa Barbara. Between 10 to 13 grains were analyzed for each of the 7 olivine populations, and one major element analysis was made on the core of each olivine. For these analyses, a 4 μm beam with a 45 nA current and a 20 kV accelerating voltage was used. A counting time of 40 seconds per element was used. The following standards were utilized for major element analysis: synthetic forsterite for Mg and Si, synthetic faylite for Fe, synthetic MnO for Mn, orthoclase (MAD-10) for Al, diopside (Chesterman) for Ca, a chromite (UC 523-9) for Cr, and synthetic Ni_2SiO_4 for Ni. A single olivine grain from AVON3-68-11 was analyzed throughout the analytical session to monitor instrument drift.

3. DATA AND OBSERVATIONS

The major element compositions of the magmatic olivines examined in this study are presented in Fig. 2. The data are compared with major element compositions in olivines from Samoan peridotite mantle xenoliths (Fig 2a; Hauri and Hart, 1994). As shown in Jackson and Shirey (2011), the olivine compositions in Samoan basalts exhibit no evidence for being xenocrystic mantle olivines. The high CaO at a given forsterite content observed in the olivines examined in this study are evidence of a magmatic origin, and the olivines are clearly not related to peridotite mantle xenolith compositions. Samples OFU-04-03 and ALIA104-04 show large variations in olivine forsterite content (olivine forsterite values of 77.6-85.1 [7.5% total variability] and 83.1-87.5 [4.4%], respectively) while other samples, like AVON3-78-1 and T25, show very little variation (83.8-84.1 [0.3%] and 84.2-85.2 [1%], respectively). Fig. 2b shows that the olivines and their host whole rocks from this study are not in Mg-Fe equilibrium. The Samoan lavas examined here generally fall below the equilibrium olivine-melt field (Roeder and Emslie, 1970), indicating that the olivines are likely cumulate in origin.

The $^{87}Sr/^{86}Sr$ data collected on olivines are presented in Table 1, along with previously published whole rock $^{87}Sr/^{86}Sr$ values for these samples. In Fig. 3, the new $^{87}Sr/^{86}Sr$ data are shown in order of increasing whole rock $^{87}Sr/^{86}Sr$. The four whole rocks with the lowest $^{87}Sr/^{86}Sr$ (i.e., <0.705)—samples T25, T33, OFU-04-03, ALIA-104-04 (from Ta'u, Ofu, and Muli seamount, respectively)—have olivine $^{87}Sr/^{86}Sr$ compositions that are similar to the whole rock. Using a delta notation ($\Delta^{87}Sr/^{86}Sr_{wholerock\text{-}olivine}$; see equation in the caption to Fig. 4), the $^{87}Sr/^{86}Sr$ of these olivines are <80 ppm different from the whole rock (Fig. 4). The six lavas with whole rock $^{87}Sr/^{86}Sr$ >0.705 exhibit greater whole rock-olivine $^{87}Sr/^{86}Sr$ disequilibrium, and the $^{87}Sr/^{86}Sr$ of the olivines in these lavas have $^{87}Sr/^{86}Sr$ that is >100 ppm different than the whole rock. With the exception of two lavas from the same dredge of Vailulu'u seamount (AVON3-63-2 and AVON3-63-11), which exhibit olivine $^{87}Sr/^{86}Sr$ ratios that are 185 and 103 ppm higher than the whole rock, the remaining lavas with $^{87}Sr/^{86}Sr$ > 0.705 (all from Vailulu'u [AVON3-73-2, AVON3-68-11, AVON3-71-2] or Malumalu [AVON3-78-1] seamounts) have olivine $^{87}Sr/^{86}Sr$ ratios that are 184 to 1947 ppm lower than the whole rock. A key observation is that the three whole rock lavas with the highest $^{87}Sr/^{86}Sr$ (AVON3-68-11, AVON3-71-2, AVON3-78-1) have the greatest wholerock-olivine $^{87}Sr/^{86}Sr$ disequilibrium. Sample AVON3-78-1, which has the highest whole rock $^{87}Sr/^{86}Sr$, shows the greatest $^{87}Sr/^{86}Sr$ disequilibrium, 1947 ppm (with replicate analyses showing 1591 and 2139 ppm).

Two Vailulu'u seamount samples (AVON3-68-11 and AVON3-71-2) have two visually distinct populations of olivines, green and brown. For both basalt samples, the green olivines have more primitive (higher) forsterite compositions and lower CaO than the brown olivines, and with no compositional (i.e., forsterite number and CaO) overlap between the two populations (Fig. 2a; supplementary Table 3). Olivine populations isolated from sample AVON3-68-11 have $^{87}Sr/^{86}Sr$ ratios that are 229 ppm (green olivines) and 489 ppm (brown olivines) lower than the whole rock. Critically, the two olivine populations from this lava—green (0.705433±0.000014, 2σ) and brown (0.705249±0.000013)—show a $^{87}Sr/^{86}Sr$ difference of 260 ppm. While the two populations of olivines separated from sample AVON3-71-2 also have lower $^{87}Sr/^{86}Sr$—718 ppm lower (brown olivines) and 763 ppm lower (green olivines)—than the whole rock, there is only a small difference (44 ppm) between the $^{87}Sr/^{86}Sr$ of the two olivine populations from this lava. Additionally, there is no clear pattern of one population (green or brown) exhibiting greater disequilibrium.

There are no obvious covariations between whole rock-olivine $^{87}Sr/^{86}Sr$ disequilibrium and average olivine compositions for each sample (supplementary Fig. 1a). Additionally, there is no relationship between whole rock-olivine $^{87}Sr/^{86}Sr$ disequilibrium and variability (given as the 1 σ standard deviation of the olivine compositions in each sample) in olivine compositions within each sample (supplementary Fig. 1b).

The available $^{87}Sr/^{86}Sr$ data for olivine-hosted melt inclusions (Jackson and Hart, 2006) and magmatic clinopyroxenes (Jackson et al., 2009) from two Samoan lavas (AVON3-78-1 and AVON3-71-2) that were analyzed for $^{87}Sr/^{86}Sr$ on aggregate olivine separates in this study are plotted in Fig. 5. Data from sample AVON3-63-2 are also shown in Fig. 6, but there are no cpx data for this lava. The olivine-hosted melt inclusions in the two Samoan lavas that exhibit the greatest whole rock-olivine $^{87}Sr/^{86}Sr$ disequilibrium (AVON3-78-1 and AVON3-71-2) tend to have lower melt inclusion $^{87}Sr/^{86}Sr$ ratios than the whole rock (Jackson and Hart, 2006). Therefore, it is not surprising that the aggregate olivine $^{87}Sr/^{86}Sr$ ratios in these two lavas are also shifted to lower $^{87}Sr/^{86}Sr$ than the whole rock. Similarly, $^{87}Sr/^{86}Sr$ ratios measured on two populations of visually distinct magmatic clinopyroxenes from both lavas are lower than the respective whole rock (Fig. 5; Jackson et al., 2009). This observation is notable, as it indicates that the two lavas with the highest $^{87}Sr/^{86}Sr$ examined in this study host a component (seen only in olivine hosted melt inclusions, aggregated olivines, and clinopyroxenes) that is less geochemically-enriched than the whole rock lava. However, in sample AVON3-63-2, the olivine has slightly higher $^{87}Sr/^{86}Sr$ than the whole rock as does the average $^{87}Sr/^{86}Sr$ of the melt inclusions.

In Fig. 6, the unweighted average $^{87}Sr/^{86}Sr$ of individual olivine-hosted melt inclusions (from Jackson and Hart, 2006) is used to calculate the $^{87}Sr/^{86}Sr$ disequilibrium between the whole rock and the melt inclusions (i.e., $\Delta^{87}Sr/^{86}Sr_{(\text{wholerock–melt inclusion average})}$; see caption of Fig. 6). The $\Delta^{87}Sr/^{86}Sr_{(\text{whole rock – melt inclusion average})}$ disequilibrium is then compared with the whole rock-olivine $^{87}Sr/^{86}Sr$ disequilibrium (i.e., $\Delta^{87}Sr/^{86}Sr_{(\text{wholerock–olivine})}$). Fig. 6 shows that the $^{87}Sr/^{86}Sr$ disequilibrium between whole rocks and average $^{87}Sr/^{86}Sr$ of the olivine-hosted melt inclusions relates positively with the $^{87}Sr/^{86}Sr$ disequilibrium between whole rocks and the aggregate olivine measurements. However, the relationship is imperfect, as AVON3-78-1 deviates from the one-to-one line. The discrepancy between the average melt inclusion $^{87}Sr/^{86}Sr$ and the aggregate olivine $^{87}Sr/^{86}Sr$ may be attributed to the limited number of individual melt inclusions $^{87}Sr/^{86}Sr$ measurements available (only 11 melt inclusions were analyzed from sample AVON3-78-1; Jackson and Hart, 2006), which is dwarfed by the large number of inclusions that were analyzed (likely 100's) in the aggregate olivine measurement. It is possible that a larger number of individual melt inclusion $^{87}Sr/^{86}Sr$ analyses would provide an average composition that better approximates the $^{87}Sr/^{86}Sr$ in the aggregate olivine analysis. Nonetheless, the rough positive relationship observed in Fig. 6 is consistent with the hypothesis that the $^{87}Sr/^{86}Sr$ ratios of aggregate olivine measurements are controlled by the Sr in the olivine-hosted melt inclusions.

Disequilibrium between $^{87}Sr/^{86}Sr$ in the whole rock and the $^{87}Sr/^{86}Sr$ in olivines varies with Cl/K measured on pillow rim glasses (Fig 7). It is necessary to analyze deeply erupted submarine glass in order to capture Cl concentrations that are relatively unaffected by degassing. Unfortunately, only three samples analyzed for whole rock and olivine $^{87}Sr/^{86}Sr$ have coexisting submarine glass. The Cl/K ratios in these samples provide important insights into the origins of the whole rock-olivine $^{87}Sr/^{86}Sr$ disequilibrium. Cl/K varies from 0.042 to 0.18 in glasses from three lavas, where relatively high Cl/K (> 0.08) in submarine volcanic glass is considered to be an indicator of the assimilation of seawater-derived materials (Michael and Schilling, 1989; Workman et al., 2006; Kendrick et al., 2013, 2015). The lava (sample AVON3-78-1) with the greatest whole rock-olivine $^{87}Sr/^{86}Sr$ disequilibrium (1947 ppm) has the lowest Cl/K ratio (0.042), which is similar to that of pristine, uncontaminated mantle melts (Stroncik and Haase, 2004). In contrast, the lava (ALIA-104-04) with the smallest magnitude whole rock-olivine $^{87}Sr/^{86}Sr$ disequilibrium (11 ppm) has the highest Cl/K (0.18). Sample AVON3-71-2 has intermediate whole rock $^{87}Sr/^{86}Sr$ disequilibrium has an intermediate Cl/K ratio (0.17). The important observation is that increased whole rock-olivine $^{87}Sr/^{86}Sr$ disequilibrium is not associated with enhanced signatures for assimilation of seawater-derived materials (i.e., higher Cl/K).

$^{3}He/^{4}He$ previously measured on Samoan olivines are plotted against $^{87}Sr/^{86}Sr$ measured in the respective whole rock (Fig 8a). In Fig. 8b, $\delta^{18}O$ previously measured on Samoan olivines are plotted against whole rock $^{87}Sr/^{86}Sr$. In both panels of Fig. 8, the effects of comparing $^{87}Sr/^{86}Sr$ measured in olivines with olivine $^{3}He/^{4}He$ and olivine $\delta^{18}O$ are also shown. In a plot of olivine $^{3}He/^{4}He$ versus olivine $^{87}Sr/^{86}Sr$, the $^{87}Sr/^{86}Sr$ of the olivines in lavas with the highest whole rock $^{87}Sr/^{86}Sr$ tend to be shifted to lower $^{87}Sr/^{86}Sr$ (than the respective whole rock) at the same $^{3}He/^{4}He$ value. When olivine $^{87}Sr/^{86}Sr$ is compared to $\delta^{18}O$ measured on olivines (Fig 8b), the slope of the correlation in olivine $^{87}Sr/^{86}Sr$ versus $\delta^{18}O$ space steepens compared to the array formed when plotting whole rock $^{87}Sr/^{86}Sr$ versus $\delta^{18}O$. In summary, the relationships between $^{87}Sr/^{86}Sr$ and $^{3}He/^{4}He$ and between $^{87}Sr/^{86}Sr$ and $\delta^{18}O$ are significantly modified when $^{87}Sr/^{86}Sr$ measurements of olivines are compared with $^{3}He/^{4}He$ and $\delta^{18}O$ measured on olivines.

4. DISCUSSION

4.1. What is the mechanism responsible for generating the whole rock-olivine $^{87}Sr/^{86}Sr$ disequilibrium: Mantle source heterogeneity versus processes operating in magma chambers?

Samoan magmatic olivines can record significantly different $^{87}Sr/^{86}Sr$ than the whole rock lava in which they are hosted, but the mechanism producing this disequilibrium is uncertain. The $^{87}Sr/^{86}Sr$ disequilibrium observed between whole rocks and bulk olivines relates to the isotopic disequilibrium between whole rocks and the average $^{87}Sr/^{86}Sr$ of the population of melt inclusions hosted in the olivines (Fig. 6). Therefore, a population of olivines in a Samoan lava must have crystallized from, and trapped, melts of different $^{87}Sr/^{86}Sr$ composition than the final erupted lava that hosts the olivines. A primary question is how melts with different $^{87}Sr/^{86}Sr$ can exist in the same magmatic plumbing system and contribute heterogeneous $^{87}Sr/^{86}Sr$ to a lava and the magmatic olivines it hosts. Here we explore two potential mechanisms for generating heterogeneous melts in magma chambers, which ultimately drive the whole rock-olivine $^{87}Sr/^{86}Sr$

disequilibrium in the Samoan samples: 1) variable assimilation of seawater-derived materials (including altered oceanic crust) and 2.) mixing of isotopically-diverse magmas sampling heterogeneous mantle sources that did not experience assimilation of seawater-derived materials.

First, however, it is important to be clear that olivines serve as capsules that preserve the Sr isotopic composition of trapped melts. For elements that have high diffusivities in olivines (e.g., Fe), diffusive exchange between the melt inclusion and the host olivine can be rapid (Gaetani and Watson, 2000). However, diffusion of Sr in olivines (log of the Sr diffusivity is $10^{-18.7}$ m^2/s at 1275°C) is quite slow (Remmert et al., 2008). The low diffusivity of Sr in olivine, together with the incompatibility of Sr in olivine (Beattie, 1994), aid the preservation of Sr-isotopic differences in olivine-hosted melt inclusions relative to the host melt. Thus, the olivine acts as a vessel effectively limiting diffusive exchange with the host melt.

4.1.1 Assimilation. The Samoan volcanoes examined here have ages of <1 Ma (Sims et al., 2008; Koppers et al., 2011). However, these young volcanoes were constructed on top of old oceanic lithosphere that has an age of ~100 Ma (Taylor, 2006). Ancient oceanic crustal lithosphere may be extensively altered by interaction with seawater. If a mantle melt assimilates altered oceanic crust and/or seawater-derived components that host radiogenic $^{87}Sr/^{86}Sr$ (e.g., Hart et al., 1999; Hauff et al., 2003), the $^{87}Sr/^{86}Sr$ of the melt will be modified. This is because seawater has higher $^{87}Sr/^{86}Sr$ (0.709179; Mokadem et al., 2015) than all Samoan lavas from the eastern region of the hotspot where the samples in this study were collected—a subset of lavas from the western region of the Samoan hotspot have $^{87}Sr/^{86}Sr$ higher than seawater, but these lavas are not examined here (Jackson et al., 2007a).

Where whole rock – olivine $^{87}Sr/^{86}Sr$ disequilibrium is observed in this study, the whole rocks tend to have higher $^{87}Sr/^{86}Sr$ than the olivine. This observation might be explained by the following assimilation scenario, which assumes that the assimilated materials have $^{87}Sr/^{86}Sr$ that is higher than identified in whole rocks in this study. If assimilation of seawater derived materials is responsible for increasing the whole rock $^{87}Sr/^{86}Sr$ relative to the olivines, then the growth of olivines must have occurred early in the evolution of a magma chamber, prior to significant assimilation of altered oceanic crust or seawater derived material. In this model, pristine melts with low $^{87}Sr/^{86}Sr$ are trapped as melt inclusions in growing olivines prior to significant assimilation. Subsequently, the remaining melt assimilates material with high $^{87}Sr/^{86}Sr$—including altered oceanic crust, seawater and/or brines—that increases the $^{87}Sr/^{86}Sr$ of the magmas. Indeed, there are indications that a small mass fraction of altered oceanic crustal sections extend to extremely radiogenic $^{87}Sr/^{86}Sr$ (up to 0.7257; Hauff et al., 2003). Melt inclusions would preserve the lower $^{87}Sr/^{86}Sr$ of the pristine (i.e., pre-assimilation) melt even as the host magma assimilates material with higher $^{87}Sr/^{86}Sr$. Olivines are an early-crystallizing phase and it is reasonable to assume that olivines will tend to trap melts very early in the history of a magma. Thus, in this simple model, magmas that have assimilated altered crustal material have high $^{87}Sr/^{86}Sr$ that is generally higher than the olivines they host. Similarly, magmas that did not experience assimilation have low $^{87}Sr/^{86}Sr$ that is similar to the olivines they host. This conceptual model provides a mechanism for generating the higher $^{87}Sr/^{86}Sr$ in whole rocks relative to their host olivines, particularly in lavas that have the highest $^{87}Sr/^{86}Sr$ (Fig. 3 and 4).

One prediction of this model is that the erupted melt (which quenches to glass or crystallizes as basaltic matrix) should have strong signatures for seawater-derived components. However, this assimilation model is inconsistent with independent indicators of assimilation, including Cl/K. Globally, Cl/K ratios are higher in oceanic lavas that have assimilated altered oceanic crust, seawater and/or brines (e.g., Michael and Schilling, 1989; Jambon et al., 1995; Kent et al., 1999a, 1999b; Lassiter et al., 2002; Stroncik and Haase, 2004; Kendrick et al., 2013). If whole rock-olivine $^{87}Sr/^{86}Sr$ disequilibrium is generated through the assimilation of seawater-derived material, increasing magnitude of whole rock-olivine $^{87}Sr/^{86}Sr$ disequilibrium should correlate with increasing Cl/K ratio. However, the Samoan lava (sample AVON3-78-1) with the largest magnitude olivine-whole rock $^{87}Sr/^{86}Sr$ disequilibrium in this study has among the lowest Cl/K (0.042, measured on a submarine pillow glass) in the Samoan suite (Fig. 7). This Cl/K is similar to that of uncontaminated primary mantle melts (Stroncik and Haase, 2004). A subset of Samoan lavas do exhibit elevated Cl/K, which is indicative of the assimilation of seawater-derived materials (Workman et al., 2006; Kendrick et al., 2015). However, the lava with the highest Cl/K (~0.18) examined in this study (sample ALIA-104-04), which is associated with higher degrees of assimilation of seawater-derived materials, shows the smallest magnitude whole rock-olivine $^{87}Sr/^{86}Sr$ disequilibrium (i.e., < 11 ppm) (Fig. 7). In summary, the relationship between Cl/K and whole rock-olivine $^{87}Sr/^{86}Sr$ disequilibrium is inconsistent with assimilation as the mechanism causing the $^{87}Sr/^{86}Sr$ disequilibrium in this sample suite.

However, the Cl/K of the pillow rim glass may not be representative of (and may record a different history than) the Cl/K in the olivine-hosted melt inclusions. In order to fully assess assimilation of seawater derived material as a mechanism for generating whole rock-olivine $^{87}Sr/^{86}Sr$ disequilibrium, both $^{87}Sr/^{86}Sr$ and an independent indicator of assimilation (i.e., Cl/K) must be measured in individual melt inclusions. It is possible that magmatic phenocrysts are more likely to crystallize near the magma chamber walls—where the magma is in contact with the cooler wall rocks of the magma chamber (Kamenetsky et al., 1998; Danyushevsky et al.,2004). Thus, compared to the bulk of an erupted lava (including liquids represented by pillow rim glass), melt inclusions may preferentially trap melts that have assimilated altered oceanic crust at the margins of a magma chamber, a process that may impart compositional and isotopic variability on melt inclusions hosted in a single erupted lava. Altered oceanic crust may not have $^{87}Sr/^{86}Sr$ that is as radiogenic as the samples with the highest whole rock $^{87}Sr/^{86}Sr$ ratios in this study. Instead, altered oceanic crust typically has $^{87}Sr/^{86}Sr$ ratios (<0.7050) that is at the low end of the range of $^{87}Sr/^{86}Sr$ observed in Samoan lavas (i.e., 0.7044). For example, Hauff et al. (2003) report average values of 0.7048 to 0.7049 in drill cores of old (130 to 167 Ma) western Pacific crust. If melt inclusions assimilated altered oceanic crust of this composition, the $^{87}Sr/^{86}Sr$ of Samoan melt inclusions will actually be reduced compared to most pristine Samoan melts, and the reduction in $^{87}Sr/^{86}Sr$ due to assimilation will be associated with higher Cl/K in the same melt inclusions. Therefore, if olivine hosted melt inclusions preferentially trap a melt (at the margins of the magma chamber) with high proportions of assimilated seawater-derived material with $^{87}Sr/^{86}Sr < 0.7050$, then the melt inclusions will tend to have higher Cl/K and lower $^{87}Sr/^{86}Sr$ than the bulk lava. In this model, however, pillow rim glasses measured in this study (which are representative of the basaltic groundmass) may not have a Cl/K ratio that is representative of the melt inclusions, because the melt inclusions may be more prone to assimilation than pillow rim glass. It is conceivable that the pillow rim glass could be pristine (e.g., AVON3-78-1 whole rock), and have low Cl/K and high $^{87}Sr/^{86}Sr$, while the melt inclusion population could inherit higher Cl/K and lower $^{87}Sr/^{86}Sr$ by assimilation. This model may be consistent with the data from, for example, AVON3-78-1, where the olivines have lower $^{87}Sr/^{86}Sr$ than the whole rock and the pillow rim glass has low Cl/K (see **Fig. 7**): If the melt inclusions from AVON3-78-1 have elevated Cl/K, the whole rock – olivine $^{87}Sr/^{86}Sr$ disequilibrium in this lava would be best explained by a crustal assimilation mechanism. Unfortunately, Cl/K data on olivine-hosted melt inclusions in the samples examined in this study are not yet available to evaluate this hypothesis.

4.1.2. Magma mixing of pristine melts that sample different mantle sources.

Magma mixing of isotopically heterogeneous melts that reflect the $^{87}Sr/^{86}Sr$ of their respective mantle sources also can generate whole rock–olivine $^{87}Sr/^{86}Sr$ disequilibrium in the

Samoan lavas examined in this study. A simple magma mixing scenario provides one possible mechanism for generating magmas that have higher $^{87}Sr/^{86}Sr$ than the olivines they host. If olivine crystallizes from a magma with low $^{87}Sr/^{86}Sr$, then melt with the same (low) $^{87}Sr/^{86}Sr$ will be trapped in the olivines as melt inclusions. If this low $^{87}Sr/^{86}Sr$ magma later mixes with an olivine-free (or olivine-poor) magma of a higher $^{87}Sr/^{86}Sr$ composition, and no further olivine is crystallized, the $^{87}Sr/^{86}Sr$ of the olivine hosted melt inclusions (and therefore, the aggregated olivines) in the final lava will be lower than the $^{87}Sr/^{86}Sr$ of the whole rock lava. Samoan lavas with high $^{87}Sr/^{86}Sr$ tend to have higher SiO_2 (and less olivine) than low $^{87}Sr/^{86}Sr$ melts (which host more olivine; Jackson et al., 2007a; see supplementary Fig. 2). Therefore, a magma that forms by mixing a high $^{87}Sr/^{86}Sr$ magma with low $^{87}Sr/^{86}Sr$ magma is likely to host an olivine cargo that originated in (and has $^{87}Sr/^{86}Sr$ that matches) the low $^{87}Sr/^{86}Sr$ magma. However, the liquid of the magma mixture will be a mixture of liquids from both magmas, and will be shifted toward the higher $^{87}Sr/^{86}Sr$ magma. While this is a simple conceptual model, it illuminates a primary observation of this study: Samoan whole rocks with the highest $^{87}Sr/^{86}Sr$ tend to host olivine with significantly lower $^{87}Sr/^{86}Sr$ than the whole rock (Fig. 3).

High SiO_2 melts with low $^{87}Sr/^{86}Sr$ do exist in the Samoan lava suite, but are relatively uncommon and they are poor in olivine. If a magma of this composition were to mix with a mafic, olivine-rich magma with higher $^{87}Sr/^{86}Sr$, then olivines in the mixed magma will host higher $^{87}Sr/^{86}Sr$ than final erupted lava. This may explain the observation that 3 out of the 10 lavas in this study host aggregate olivines with higher $^{87}Sr/^{86}Sr$ than the whole rock.

We employ a simple binary mixing model to show how mixing between mafic, low $^{87}Sr/^{86}Sr$ melts and high SiO_2, high $^{87}Sr/^{86}Sr$ melts can generate the whole rock – olivine $^{87}Sr/^{86}Sr$ disequilibrium observed here. The whole rock and olivine $^{87}Sr/^{86}Sr$ data from Samoan sample AVON3-71-2 are used as an example to illustrate this process. In the model we assume that the

AVON3-71-2 whole rock $^{87}Sr/^{86}Sr$ composition is the result of mixing a melt with low $^{87}Sr/^{86}Sr$ (represented by the average $^{87}Sr/^{86}Sr$ of the bulk olivines from this lava) and a silicic, olivine-free melt with high $^{87}Sr/^{86}Sr$ (represented by Samoan sample ALIA-115-21). The low average $^{87}Sr/^{86}Sr$ of the melts trapped in the bulk olivines from AVON3-71-2 (i.e., 0.705420) is used in the mixing calculation, and the Sr concentration of the endmember melt trapped in the olivines is given by the average Sr concentration of the olivine-hosted melt inclusions from this sample (484 ppm; Jackson and Hart, 2006). The high $^{87}Sr/^{86}Sr$ (0.720469) of the SiO_2-rich (and olivine free) Samoan lava ALIA-115-21 is used for the enriched endmember in the mixing calculation, which has [Sr] of 478 ppm (Jackson et al. 2007a). Given these model input parameters, the $^{87}Sr/^{86}Sr$ of AVON3-71-2 is generated by adding 3.5% of ALIA115-21 melt to 96.5% of a melt like that sample by AVON3-71-2 olivines. If the olivines crystalized from the mafic endmember prior to mixing, thereby trapping the $^{87}Sr/^{86}Sr$ ratio measured in the AVON3-71-2 olivines, then the melt in the final mixture will have $^{87}Sr/^{86}Sr$ that is higher (0.705943) than the olivines.

However, it is important to recognize that magma mixing scenarios can be more complex, and olivine likely crystallizes over a longer portion of the magma's evolution. For example, if olivine crystallizes from a magma before and after mixing with other, isotopically heterogeneous magmas, the individual olivine hosted melt inclusions will record the history of mixing in the system. If a mafic magma with relatively high $^{87}Sr/^{86}Sr$ is mixed into a magma system while olivine is being crystallized, the melt inclusions will record the increasing $^{87}Sr/^{86}Sr$ composition of the melt. If a low $^{87}Sr/^{86}Sr$ mafic melt is later mixed into the system, newly-crystallizing olivine can trap melt inclusions that record the subsequent decrease in the $^{87}Sr/^{86}Sr$ of the bulk melt. The final olivine population would include melt inclusions with both higher and lower $^{87}Sr/^{86}Sr$ than the final erupted lava, while the measurements of $^{87}Sr/^{86}Sr$ in pooled olivines provide an average $^{87}Sr/^{86}Sr$ composition of the melt for the period during which olivines were crystallizing. This scenario may help explain the distribution of $^{87}Sr/^{86}Sr$ in melt inclusions from Samoan sample AVON3-68-3 (see Jackson and Hart, 2006), which has melt inclusions that are both higher and lower $^{87}Sr/^{86}Sr$ than the whole rock, while the unweighted average melt inclusion $^{87}Sr/^{86}Sr$ and the aggregate olivine $^{87}Sr/^{86}Sr$ compositions are lower than the whole rock.

4.1.3. A hybrid model: magma mixing and assimilation.

An important question is how magmas with different $^{87}Sr/^{86}Sr$ occupy the same magma plumbing system so that they can mix. One possibility is that the two pristine magmas sample two different mantle sources with different $^{87}Sr/^{86}Sr$. Alternatively, the magmas may inherit heterogeneous $^{87}Sr/^{86}Sr$ by assimilation of altered oceanic crust, and these heterogeneous magmas then mix to generate the diversity of $^{87}Sr/^{86}Sr$ recorded in erupted lavas and the olivine they host. Again, measurements pairing $^{87}Sr/^{86}Sr$ and Cl/K in individual melt inclusions will provide important insights into the mechanism driving the whole rock – olivine $^{87}Sr/^{86}Sr$ disequilibrium observed in this study. If the melt inclusions have low, mantle-like Cl/K that is unrelated to $^{87}Sr/^{86}Sr$, then mixing of pristine melts with heterogeneous $^{87}Sr/^{86}Sr$ is likely to be generating the intra-lava $^{87}Sr/^{86}Sr$ disequilibrium. Alternatively, if melt inclusions Cl/K is variable and correlates with melt inclusions $^{87}Sr/^{86}Sr$ in the same lava, then crustal assimilation is likely influencing the whole rock olivine $^{87}Sr/^{86}Sr$ disequilibrium. Future studies targeting individual melt inclusions for paired Cl/K and $^{87}Sr/^{86}Sr$ measurements will be critical for determining the origin of the whole rock-olivine $^{87}Sr/^{86}Sr$ disequilibrium.

Finally, it is important to note that, if the conceptual magma mixing model for the origin of whole rock-olivine $^{87}Sr/^{86}Sr$ disequilibrium in Samoan lavas is correct, olivines with different $^{87}Sr/^{86}Sr$ than the host lavas are not phenocrysts, as the olivines with different $^{87}Sr/^{86}Sr$ could not have crystallized from the same lava. However, these olivines are not xenocrysts either, because they crystallized from melts that mixed to generate the final erupted lava. The term antecrysts (Hildreth, 2001; Charlier et al., 2005; Gill et al., 2006; Davidson et al., 2007) may best describe the olivines in the Samoan lavas that exhibit $^{87}Sr/^{86}Sr$ disequilibrium with the whole rock. Antecrysts differ from phenocrysts in that, instead of crystallizing from the erupted lava, they crystallized from progenitors of the final erupted melt. Antecrysts are also not xenocrysts as they are derived directly from the active plumbing system, possibly after multiple magma replenishment events (Jerram and Martin, 2008).

4.2. Mass balance for the $^{87}Sr/^{86}Sr$ in the olivines and the whole rock.

The majority of the magmatic olivines in this study have lower $^{87}Sr/^{86}Sr$ than the whole rock host (Fig. 3). Therefore, in these lavas, there must exist a component with higher $^{87}Sr/^{86}Sr$ than the whole rock in order to mass balance the elevated $^{87}Sr/^{86}Sr$ measured within the lava. The simplest explanation is that basalt matrix has slightly higher $^{87}Sr/^{86}Sr$ than the whole rock, thus balancing the lower $^{87}Sr/^{86}Sr$ in the olivine separates (where the "whole rock" represents all the constituents in a lava, including magmatic phases [i.e., olivine and cpx] and basaltic matrix). We use Samoan sample AVON3-78-1 (Fig. 5) to illustrate the magnitude of elevation of $^{87}Sr/^{86}Sr$ required in the basalt matrix to balance the low $^{87}Sr/^{86}Sr$ of the olivines. In this calculation, the whole rock $^{87}Sr/^{86}Sr$ and Sr concentration is a mixture of basalt matrix, cpx, and olivine, and thus the whole rock composition must have an $^{87}Sr/^{86}Sr$ and Sr concentration that is between the endmembers. The $^{87}Sr/^{86}Sr$ (0.708901) and Sr concentration (333ppm) of the whole rock are known (Workman et al., 2004). Similarly, the $^{87}Sr/^{86}Sr$ (0.707521; this study), Sr concentration (0.26 ppm; this study) and modal abundance of the olivine (25%; Workman et al., 2004) are known. Additionally, the $^{87}Sr/^{86}Sr$ (0.707985, average two cpx populations from Jackson et al., 2009), Sr concentration (44 ppm, calculated by averaging measured concentrations from Jackson et al., 2009) and modal abundance of the cpx (5%; Workman et al., 2004) are known. Thus, only 0.02% of the whole rock Sr is hosted in the olivines. The modal abundance of matrix (i.e., 100% - 25% - 5% = 70%) is also known, leaving the basalt matrix $^{87}Sr/^{86}Sr$ and Sr concentration as the only remaining unknowns. The Sr concentration of the whole rock is the sum of the products of the Sr concentrations and modal abundances of the phases present (i.e. cpx, olivine, and matrix), which allows calculation of the Sr concentration of the matrix, which is 472 ppm. The $^{87}Sr/^{86}Sr$ of the whole rock is the sum of the matrix, cpx, and olivine $^{87}Sr/^{86}Sr$, weighted by the fraction of the whole rock Sr that is hosted in each component, matrix, cpx, and olivine. Given these constraints, an $^{87}Sr/^{86}Sr$ ratio in the matrix that is only 9 ppm greater than that of the whole rock is required to balance the lower $^{87}Sr/^{86}Sr$ of the olivine and cpx cargo. This mass balance calculation demonstrates that the lower olivine $^{87}Sr/^{86}Sr$ does not strongly influence the $^{87}Sr/^{86}Sr$ of the whole rock owing to the much higher concentration of Sr in the matrix compared to the olivines.

4.3. Sr-isotopes in olivines: implications for redefining relationships between isotopes traditionally measured in olivines (e.g., $^{3}He/^{4}$*He and* $\partial^{18}O$) and isotopes measured in whole rocks (e.g. $^{87}Sr/^{86}Sr$).

4.3.1. Olivine $^{3}He/^{4}He$ versus olivine $^{87}Sr/^{86}Sr$.

Relationships between helium isotope and heavy radiogenic isotopes, like $^{87}Sr/^{86}Sr$, have long been used to constrain the evolution and structure of the mantle (e.g, Kurz et al., 1982; Zindler and Hart, 1986; Hart et al., 1992; Graham, 2002; Allègre and Moreira, 2004; Class and Goldstein, 2005). However, measurements of heavy radiogenic isotopes, including $^{87}Sr/^{86}Sr$, are often carried out on whole rock basalt powders (e.g., Hofmann, 1997; Stracke et al., 2005; White, 2010, 2015). Whole rocks are unsuitable for measuring helium isotopes, so ^{3}He/^{4}He is often measured on magmatic olivines separated from the lava (olivine-hosted melt inclusions contain less degassed melts suitable for helium isotopic measurement). Olivine ^{3}He/^{4}He data are then compared with the isotopic ratios of other elements (e.g., ^{87}Sr/^{86}Sr) measured in a whole rock. This approach is robust provided the ^{87}Sr/^{86}Sr measured in the whole rock powder is the same as the ^{87}Sr/^{86}Sr in the olivine. However, the results of this study show that olivines can have different ^{87}Sr/^{86}Sr than the whole rock.

In olivines, incompatible elements like He (Parman et al., 2005; Heber et al., 2007; Jackson et al., 2013) and Sr are hosted primarily in melt inclusions. Therefore, pooling olivines for ^{87}Sr/^{86}Sr analysis is advantageous as it permits direct comparison of the two isotopic systems in the same material (i.e, the population of melt inclusions hosted in the olivines). Unfortunately, measuring both ^{3}He/^{4}He and ^{87}Sr/^{86}Sr within a single olivine-hosted melt inclusion is beyond current analytical capabilities. Nonetheless, the different ^{87}Sr/^{86}Sr between Samoan whole rocks and the olivines they host has the potential to modify established relationships between ^{3}He/^{4}He and ^{87}Sr/^{86}Sr.

When olivine ^{3}He/^{4}He is compared with whole rock ^{87}Sr/^{86}Sr, the Samoan lava suite forms a “wedge shape” (Fig. 8a): high ^{3}He/^{4}He appears only in lavas with low ^{87}Sr/^{86}Sr, and low ^{3}He/^{4}He appears in lavas with both high ^{87}Sr/^{86}Sr and low ^{87}Sr/^{86}Sr. However, samples with the highest whole rock ^{87}Sr/^{86}Sr tend to have olivines with significantly lower ^{87}Sr/^{86}Sr (Figs 3 and 4). Therefore, when olivine ^{3}He/^{4}He is compared with olivine ^{87}Sr/^{86}Sr, a somewhat different relationship between these two isotopic systems emerges. For example, for the three lavas that exhibit the largest whole rock-olivine ^{87}Sr/^{86}Sr disequilibrium (AVON3-78-1, AVON3-71-2, and AVON3-68-11), the ^{87}Sr/^{86}Sr data are effectively shifted to lower values when olivine data are used (Fig. 8). This shift in the olivine $^{87}Sr/^{86}Sr$ data can be described by simple binary mixing between a low $^{3}He/^{4}He$ melt that is helium rich and a high $^{3}He/^{4}He$ melt that is helium poor (Fig. 8a). If a melt with the Sr and He isotopic compositions of Ofu-04-06 (0.704584; 33.8 Ra) is mixed with a melt with the isotopic compositions of AVON3-78-1(0.708901; 8.22 Ra), and if (at the time of mixing) the AVON3-78-1 melt had a helium concentration thirty times that of the Ofu 04-06, then the mixing line between the two endmembers describes how olivines hosted in the whole rocks with the highest $^{87}Sr/^{86}Sr$ can be shifted to lower $^{87}Sr/^{86}Sr$ than the whole rock (while preserving a similar $^{3}He/^{4}He$). However, this requires that the olivines tend to sample a larger fraction of the low $^{87}Sr/^{86}Sr$ component than the whole rock (Fig. 8a).

Over the past several decades, a significant body of work has systematically related noble gas and lithophile radiogenic isotopic systems (e.g., Kurz et al., 1982; Farley et al., 1992; Hart et al., 1992; Hanan and Graham, 1996; Graham, 2002; Class and Goldstein, 2005; Caro and Bourdon, 2010). This is critical, as "chemical geodynamics" (e.g., Zindler and Hart, 1986) is built upon hypotheses that attempt to relate different isotopic systems—including $^{3}He/^{4}He$, $^{87}Sr/^{86}Sr$—measured in mantle-derived lavas. Thus, determining relationships between $^{3}He/^{4}He$ and $^{87}Sr/^{86}Sr$ in the source magma is essential for developing a more complete understanding of the geodynamic evolution of the mantle. We argue that analysis of He and Sr in olivines provides a direct comparison of the two systems that have important implications for global OIB systematics between $^{3}He/^{4}He$ and $^{87}Sr/^{86}Sr$.

Analysis of $^{3}He/^{4}He$ and $^{87}Sr/^{86}Sr$ in deeply-dredged submarine volcanic glasses—which represent less degassed magma compositions—can circumvent the issue posed by whole rock-olivine $^{87}Sr/^{86}Sr$ disequilibrium, as He and Sr are measured in the same homogeneous, glassy material. Unfortunately, deeply dredged submarine glasses are not available for most OIB localities, including many Samoan volcanoes, and the community has relied on $^{3}He/^{4}He$ analyses of olivines hosted in basalts at many OIB localities for decades (e.g., Kurz et al., 1982).

While whole rock-olivine $^{87}Sr/^{86}Sr$ disequilibrium can modify relationships between $^{3}He/^{4}He$ and $^{87}Sr/^{86}Sr$ in Samoan lavas, there are additional mechanisms that may decouple these two radiogenic isotopic systems. For example, post-eruptive radiogenic ingrowth of ^{4}He can rapidly and dramatically reduce the $^{3}He/^{4}He$ in erupted lavas (particularly highly degassed lavas) compared to the mantle source $^{3}He/^{4}He$ (e.g., Zindler and Hart, 1986), thereby decoupling the relationship between $^{3}He/^{4}He$ from $^{87}Sr/^{86}Sr$ measured in lavas from the relationship in the mantle source. Additionally, highly degassed lavas with low ^{4}He concentrations are susceptible to atmospheric contamination, which can decouple $^{3}He/^{4}He$ from $^{87}Sr/^{86}Sr$ (Hilton et al., 1995). Furthermore, helium has a much higher diffusivity in olivines (e.g., Hart, 1984; Trull et al., 1991) than heavy radiogenic isotopes (like Sr), and this can potentially result in diffusive decoupling of $^{3}He/^{4}He$ from $^{87}Sr/^{86}Sr$ in the mantle (e.g., Hart et al., 2008; Albarède, 2008) and in olivine hosted melt inclusions in magma chambers (Kurz et al., 2004). Whole rock-olivine $^{87}Sr/^{86}Sr$ disequilibrium identified in this study provides an additional novel mechanism for modifying relationships between $^{3}He/^{4}He$ and $^{87}Sr/^{86}Sr$.

***4.3.2. Olivine* ∂^{18}O versus olivine ^{87}Sr/^{86}Sr.** $\partial^{18}O$ is commonly measured in olivine in OIB samples, including Samoan lavas (Eiler, 2001; Widom and Farquhar, 2003; Bindeman, 2008). Therefore, whole rock-olivine $^{87}Sr/^{86}Sr$ disequilibrium in Samoan lavas also has the potential to modify established relationships between $\partial^{18}O$ and $^{87}Sr/^{86}Sr$. The published correlation between Samoan olivine $\partial^{18}O$ and whole rock $^{87}Sr/^{86}Sr$ (Workman et al., 2008) is strongly influenced by lavas with the highest $^{87}Sr/^{86}Sr$ and the highest olivine $\partial^{18}O$ (Fig. 8b), but we find that Samoan lavas with the highest whole rock $^{87}Sr/^{86}Sr$ also have the most extreme whole rock-olivine

$^{87}Sr/^{86}Sr$ disequilibrium. Thus, when the new olivine $^{87}Sr/^{86}Sr$ data are compared with olivine $\partial^{18}O$, the linear regressions through the data have a steeper slope than the Workman et al. (2008) correlation (Fig. 8b). This is important, as the slope defining the relationship between $\partial^{18}O$ and $^{87}Sr/^{86}Sr$ in Samoan lavas is critical for determining the origin of the enriched protolith contributing to the Samoan mantle. Workman et al. (2008) indicated that steeper slopes in $\partial^{18}O$-$^{87}Sr/^{86}Sr$ space are more easily fit by a recycled continental crust protolith, while shallower slopes are better fit with recycled marine sediment with a terrigenous origin. Thus, $^{87}Sr/^{86}Sr$ measurements in olivine not only have the potential to inform on relationships between isotopes measured in olivines (e.g., $\partial^{18}O$) and whole rocks ($^{87}Sr/^{86}Sr$), but also to impact existing interpretations regarding the origin of isotopic variability in the Samoan mantle. The significance of comparing whole rock $^{87}Sr/^{86}Sr$ with olivine $^{3}He/^{4}He$ and olivine $\delta^{18}O$ has to be reconsidered if whole rocks lavas and the olivines they host have different $^{87}Sr/^{86}Sr$. However, additional data pairing olivine $^{87}Sr/^{86}Sr$ with olivine $^{3}He/^{4}He$ and $\delta^{18}O$ on a larger number of samples will be important for evaluating whether the whole rock-olivine disequilibria observed in this study are representative of the Samoan suite.

4.3.3. Looking ahead: Additional radiogenic isotopic systems in olivines. In an earlier study **(**Jackson and Shirey, 2011), a subset of the Samoan lavas characterized for olivine $^{3}He/^{4}He$ (T25, T33, AVON3-63-11, AVON3-63-2, AVON3-78-1) were also characterized for both whole rock and olivine $^{187}Os/^{188}Os$. In addition to Sr and Os isotopes, it may be possible to measure other radiogenic isotopic systems in magmatic olivines. For example, Nd concentrations in olivines tend to be 10 to 20 times lower than Sr concentrations in Samoan lavas, and given the Sr measured in the olivine separates in this study (14 to 100 ng), we would expect 0.7 to 10 ng of Nd in the same aliquots of Samoan olivine (assuming that Samoan basalts and olivine hosted melt inclusions have similar Sr/Nd ratios). Thus, the potential exists to routinely measure

$^{143}Nd/^{144}Nd$ precisely in olivine separates from most Samoan samples (Koornneef et al. 2015; Harvey and Baxter, 2009). However, low abundances of certain trace elements, including Pb, may prove to be an obstacle for isotopic measurement in olivines by TIMS, but the potential exists for high precision Pb isotope measurements by SIMS (Saal et al., 1998, 2005; Maclennan, 2008) prior to destructive Sr and Nd isotopic measurements by TIMS. Nd/Pb is a canonical ratio in oceanic lavas (Hofmann, 2003), and the average Nd/Pb (15.1 ± 4.7 1σ) ratio in basaltic lavas from the volcanoes considered in this study indicate that Pb concentrations are likely to be 10 to 20 times lower than Nd concentrations in melt inclusions. Thus, Pb abundances are estimated to be only 0.033 to 1.0 ng in the olivine samples examined here, and procedural blanks may present a hurdle for routine Pb-isotopic analyses of most olivines.

Figure captions.

Figure 1. Map of Samoan volcanoes and $^{143}Nd/^{144}Nd$ versus $^{87}Sr/^{86}Sr$ in Samoan whole-rock lavas. Samoan whole rock $^{87}Sr/^{86}Sr$ and $^{143}Nd/^{144}Nd$ data are from White and Wright (1987); Farley et al. (1992), Workman et al. (2004), Jackson et al. (2007a, 2007b, 2010). Data for the global MORB and OIB data compiled from the GEOROC database (http://georoc.mpch-mainz.gwdg.de)."

Figure 2. (a) Major element compositions of the Samoan magmatic olivines examined in this study are different from the compositions of olivines analyzed in Samoan peridotite mantle xenoliths. Samoan magmatic olivine data are from this study and from Jackson and Shirey (2011). The Samoan peridotite mantle xenolith olivines are from Hauri and Hart (1994). (b) Olivine forsterite compositions are compared to the Mg number of their host whole rocks (after Garcia et al., 1995). The equilibrium field is from Roeder and Emslie (1970; Mg# = molar ratio of [Mg/(Mg + 0.9 * FeO)*100]) Whole rock major element data used for Mg-number calculation are from Workman et al. (2004).

Figure 3. Comparison of olivine and whole rock $^{87}Sr/^{86}Sr$ for 12 olivine separates from 10 Samoan basalts. The $^{87}Sr/^{86}Sr$ of the olivines (green symbols) can have different $^{87}Sr/^{86}Sr$ from the whole rock (grey symbols): In general, the difference is greatest in whole rocks with the highest $^{87}Sr/^{86}Sr$. Two visually-distinct populations of olivine were separated from two whole rocks (AVON3-71-2 and AVON3-68-11) for $^{87}Sr/^{86}Sr$ analyses. The bracket links the two replicate measurements for AVON3-78-1. Individual volcano names are provided in parentheses.

Figure 4. The relative difference in $^{87}Sr/^{86}Sr$ between the whole rock and olivine is expressed in ppm as $\Delta^{87}Sr/^{86}Sr_{\text{(wholerock - olivine)}}$ and is plotted as a function of whole rock $^{87}Sr/^{86}Sr$. Error bars are smaller than data points. $\Delta^{87}Sr/^{86}Sr_{\text{(wholerock - olivine)}} = 10^6 * (^{87}Sr/^{86}Sr_{\text{wholerock}} - {}^{87}Sr/^{86}Sr_{\text{olivine}})/ {}^{87}Sr/^{86}Sr_{\text{wholerock}}$. The bracket links the two replicate measurements for AVON3-78-1

Figure 5. Pervasive $^{87}Sr/^{86}Sr$ disequilibrium in three Samoan lavas. Whole rock $^{87}Sr/^{86}Sr$ (Workman et al., 2004) is compared with $^{87}Sr/^{86}Sr$ in olivine-hosted melt inclusions (Jackson and Hart, 2006), magmatic clinopyroxenes (Jackson et al., 2009a) and aggregated olivine separates

(this study). Excluding melt inclusions, error bars are smaller than the symbols. The bracket links the two replicate measurements for AVON3-78-1. The red circle represents the unweighted average $^{87}Sr/^{86}Sr$ of the olivine hosted melt inclusions.

Figure 6. Whole rock - olivine $^{87}Sr/^{86}Sr$ disequilibrium is compared with the $^{87}Sr/^{86}Sr$ disequilibrium between whole rocks and the unweighted average melt inclusions in the three Samoan basalts. Only three Samoan basalts (AVON3-78-1, AVON3-71-2, AVON3-63-2) have $^{87}Sr/^{86}Sr$ measured on both the aggregate olivine (this study) and on individual olivine melt inclusions (Jackson and Hart, 2006). The values for $\Delta^{87}Sr/^{86}Sr_{(\text{wholerock – olivine})}$ and $\Delta^{87}Sr/^{86}Sr_{(\text{whole rock – melt inclusion average})}$ are expressed in ppm. The "melt inclusion average" is the unweighted mean of the $^{87}Sr/^{86}Sr$ measured in olivine-hosted melt inclusions in a single basalt sample (see Jackson and Hart, 2006**)**. The $^{87}Sr/^{86}Sr$ disequilibrium between the whole rock and the melt inclusion average is calculated in the following way: $\Delta^{87}Sr/^{86}Sr_{(\text{wholerock – melt inclusion average})} = 10^6 * (^{87}Sr/^{86}Sr_{\text{wholerock}} - {}^{87}Sr/^{86}Sr_{\text{melt inclusion average}})/ {}^{87}Sr/^{86}Sr_{\text{wholerock}}$.

Figure 7. Cl/K versus $\Delta^{87}Sr/^{86}Sr_{(\text{wholerock – olivine})}$. Cl/K is available on only a small subset of samples with paired whole rock-olivine $^{87}Sr/^{86}Sr$ data in this study (ALIA-104-04, AVON3-71-2, AVON3-78-1). The grey field encompasses data from this study.

Figure 8. $^{87}Sr/^{86}Sr$ (in whole rocks and olivines) versus olivine $^3He/^4He$ (a) and olivine $\partial^{18}O$ (b). Data are for Samoan lavas only. All $^3He/^4He$ and $\partial^{18}O$ are measured in olivines. Green symbols represent samples where $^{87}Sr/^{86}Sr$ is measured in olivines, and a red line links these measurements with the corresponding whole rock $^{87}Sr/^{86}Sr$ measurement (represented by grey symbols with black lines). Grey symbols with grey lines represent Samoan samples for which

olivine $^{87}Sr/^{86}Sr$ has not yet been measured. $^{87}Sr/^{86}Sr$ error bars are smaller than the symbols. The bracket links the two replicate measurements for AVON3-78-1. The blue line in (a) is the mixing model described in section 4.3.1. Each tick mark represents a 10% fraction. The linear regressions in (b) are calculated using only data that has paired whole rock-olivine $^{87}Sr/^{86}Sr$.

Acknowledgements. We acknowledge discussion with Forrest Horton, Alison Price, Rick Carlson, and Frank Ramos. Bob Cliff's analytical assistance with Sr-isotopic measurements made at Leeds is also greatly appreciated. We acknowledge inspiration from a colleague who posited that whole rock analyses provide all the information necessary to understand the geochemistry of hotspot volcanoes. We thank Stan Hart for providing us with whole rock major element compositions for two lavas examined in this study. We acknowledge reviews from Bill White and two anonymous referees. We thank Ethan Baxter for use of the TIMS facility and clean labs at Boston University. We acknowledge support from NSF grants EAR-1348082, EAR-1347377, OCE-1153894, EAR-1145202.

References

Albarède, F., 2008. Rogue mantle helium and neon, Science 319, 943–945.

Allègre, C.J., Moreira, M., 2004. Rare gas systematics and the origin of oceanic islands: the key role of entrainment at the 670 km boundary layer. Earth Planet. Sci. Lett. 228, 85-92.

Bindeman, I. (2008). Oxygen isotopes in mantle and crustal magmas as revealed by single crystal analysis. Rev. Mineral. Geochem. 69:445-478

Beattie, P., 1994. Systematics and energetics of trace-element partitioning between olivine and silicate melts: implications for the nature of mineral/melt partitioning. Chem. Geol. 117: 57-71

Caro, G., Bourdon, B., 2010. Non-chondritic Sm/Nd ratio in the terrestrial planets: consequences for the geochemical evolution of the mantle–crust system. Geochim. Cosmochim. Acta 74, 3333–3349.

Charlier, B.L.A.,Wilson, C.J.N., Lowenstern, J.B., Blake, S., Van Calsteren, P.W., Davidson, J.P., 2005. Magma generation at a large, hyperactive silicic volcano (Taupo, New Zealand) revealed by U – Th and U – Pb systematics in zircons. J. Petrol. 46, 3–32.

Class, C., Goldstein, S.L.,2005. Evolution of helium isotopes in the Earth's mantle. Nature, 436, 1107–1112.

Danyushevsky, L.V., Leslie, R.A.J., Crawford, A.J., Durance, P., 2004. Melt inclusions in primitive olivine phenocrysts: the role of localized reaction processes in the origin of anomalous compositions. J. Pet., 45, 2531–2553.

Davidson, J.P., Morgan, D.J., Charlier, B.L.A., Harlou, R., Hora, J., 2007. Tracing magmatic processes and timescales through mineral-scale iso- topic data. An. Rev. Earth and Plan. Sci. 35, 273–311.

Eiler, J.M., 2001. Oxygen isotope variations of basaltic lavas and upper mantle rocks. In: Valley J.W., Cole D.R. (eds) Stable isotope geochemistry, Rev. Mineral. Geochem. 43, 319–364

Farley, K.A., Natland, J.H., Craig, H., 1992. Binary mixing of enriched and undegassed (primitive?) mantle components (He, Sr, Nd, Pb) in Samoan lavas. Earth Planet. Sci. Lett. 111, 183–199.

Gaetani, G.A., Watson, E.B., 2000. Open system behavior of olivine hosted melt inclusions. Earth Planet. Sci. Lett. 183, 27 – 41.

Garcia, M. O., Foss, D. J. P., West, H. B. & Mahoney, J., 1995. Geochemical and isotopic evolution of Loihi Volcano, Hawaii. J. of Petrol. 36, 1647–1674.

Gast, P.W., Tilton, G.R., Hedge, C., 1964. Isotopic composition of lead and strontium from Ascension and Gough Islands. Science 142, 1181–1185.

Gill, J., Reagan, M., Tepley, F., Malavassi, E., 2006. Introduction to Arenal volcano, Costa Rica. Magma Genesis and Volcanological Processes. J. Volcanol. Geothermal Res. 157, 1–8.

Graham, D.W., 2002. Noble gas isotope geochemistry of mid-ocean ridge and ocean island basalts; characterization of mantle source reservoirs. In: Porcelli, D., Ballentine, C.J., Wieler, R. (Eds.), Noble Gases in Geochemistry and Cosmochemistry. Rev. in Min. Geochem., 47, 247–318.

Hanan, B.B., Graham, D.W., 1996. Lead and helium isotope evidence from oceanic basalts for a common deep source of mantle plumes. Science. 272, 991–995.

Harlou, R., Pearson, D.G., Nowell, G.M., Ottley, C.J., Davidson, J.P., 2009. Combined Sr isotope and trace element analysis of melt inclusions at sub-ng levels using micro-milling, TIMS and ICPMS. Chem. Geol. 260, 254–268.

Hart, S. R., 1984. Helium diffusion in olivine. Earth Planet. Sci. Lett. 70, 297-302

Hart, S.R., Hauri, E.H., Oschmann, L.A.,Whitehead, J.A., 1992. Mantle plumes and entrainment: isotopic evidence. Science 256, 517–520.

Hart, S.R., Blusztajn, J., Dick, H.J.B., Meyer, P.S., Muehlenbachs, K., 1999. The fingerprint of seawater circulation in a 500-meter section of ocean crust gabbros. Geochim. Cosmochim. Acta, 63, 4059–4080.

Hart, S.R., Staudigel, H., Koppers, A.A.P., Blusztajn, J., Baker, E.T., Workman, R., Jackson, M., Hauri, E., Kurz, M., Sims, K., Fornari, D., Saal, A., Lyons, S., 2000. Vailulu'u Undersea Volcano: The New Samoa, Geochem, Geophys. Geosys GC000108, 1-13. DOI: 10.1029/2000GC000108

Hart, S.R., Kurz, M.D., Wang, Z., 2008. Scale length of mantle heterogeneities: constraints from helium diffusion. Earth Planet. Sci. Lett. 269, 508–517.

Hart, S. R., Jackson, M.G., 2014. Ta'u and Ofu/Olosega volcanoes: The ‘‘twin sisters’’ of Samoa, their P, T, X melting regime, and global implications, Geochem. Geophys. Geosyst 15, 2301–2318. DOI: 10.1002/2013GC005221

Harvey, J., Baxter, E.F., 2009. An improved method for TIMS high precision neodymium isotope analysis of very small aliquots (1–10 ng). Chem. Geol. 258, 251–257.

Hauff, F., Hoernle, K., Schmidt, A., 2003. Sr-Nd-Pb composition of Mesozoic Pacific oceanic crust (Site 1149 and 801, ODP Leg 185): Implications for alteration of ocean crust and the input into the Izu-Bonin-Mariana subduction system. Geochem. Geophys. Geosyst. 4, 8913 DOI:10.1029/2002GC000421

Hauri E. H., Hart S. R., 1994. Constraints on melt migration from mantle plumes: A trace element study of peridotite xenoliths from Savai'i, Western Samoa. J. Geophys. Res. 99, 24301–24321.

Heber, V.S., Brooker, R.A., Kelley, S.P., Wood, B.J., 2007. Crystal melt partitioning of noble gases (helium, neon, argon, krypton, and xenon) for olivine and clinopyroxene. Geochim. Cosmochim. Acta 71, 1041–1061.

Hildreth, W., 2001. Longevity and Dynamics of Rhyolitic Magma Systems. Penrose Conference.

Hilton D. R., Barling J., and Wheller G. E., 1995. Effect of shallow level contamination on the helium isotope systematics of ocean island lavas. Nature 373, 330-333.

Hofmann, A.W., 1997. Mantle geochemistry: The message from oceanic volcanism. Nature, 385, 219–229.

Hofmann, A.W., 2003. Sampling mantle heterogeneity through oceanic basalts: Isotopes and trace elements, in Treatise on Geochemistry: The Mantle and Core, edited by R.W. Carlson, H. D. Holland, and K.K. Turekian, pp. 61–101, Elsevier, New York

Jackson, C.R.M., Parman, S.W., Kelley, S.P., Kelley, R.F., 2013. Constraints on light noble gas partitioning at the conditions of spinel-peridotite melting. Earth Planet. Sci. Lett. 384, 178-187.

Jackson, M.G., Hart, S.R., 2006. Strontium isotopes in melt inclusions from Samoan basalts: Implications for heterogeneity in the Samoan plume. Earth Planet. Sci. Lett. 245, 260-277.

Jackson, M.G., Hart, S.R., Koppers, A.A.P., Staudigel, H., Konter, J., Blusztajn, J., Kurz, M.D., Russell, J.A., 2007a. The return of subducted continental crust in Samoan lavas. Nature, 448, 684-687.

Jackson, M.G., Kurz, M.D., Hart, S.R., Workman, R.K., 2007b. New Samoan lavas from Ofu Island reveal a hemispherically heterogeneous high ^{3}He/^{4}He mantle. Earth Planet. Sci. Lett. 264, 360–374.

Jackson, M.G., Hart, S.R., Saal, A.E., Shimizu, N., Kurz, M.D., Blusztajn, J., Skovgaard, A., 2008. Globally elevated titanium, tantalum, and niobium (TITAN) in ocean island basalts with high ^{3}He/^{4}He. Geochem. Geophys. Geosyst. 9. doi:10.1029/2007GC001876.

Jackson, M.G., Hart, S.R., Shimizu, N., Blusztajn, J., 2009. Pervasive cpx-whole rock isotopic disequilibrium in Polynesian hotspot lavas: Evidence supporting isotopic variability in olivine and clinopyroxene-hosted melt inclusions. Geochem. Geophys. Geosys. 10, Q03006, doi:10.1029/2008GC002324

Jackson, M.G., Kurz, M.D., Hart, S.R., 2009. Helium and neon isotopes in phenocrysts from Samoan lavas: evidence for heterogeneity in the terrestrial high 3He/4He mantle. Earth Planet. Sci. Lett. 287, 519–528

Jackson, M.G., Hart, S.R., Konter, J.P., Koppers, A.A.P., Staudigel, H., Kurz, M.D., Blusztajn, J., Sinton, J.M., 2010. The Samoan hotspot track on a "hotspot highway": Implications for mantle plumes and a deep Samoan mantle source. Geochem. Geophys. Geosyst. 11, Q12009, doi:10.1029/2010GC003232

Jackson, M.G., Shirey, S., 2011. Re-Os systematics in Samoan shield lavas and the use of Os-isotopes in olivine phenocrysts to determine primary magmatic compositions. Earth Planet. Sci. Lett. 312, 91-101.

Jambon, A., Deruelle, B., Dreibus, G., Pineau, F., 1995. Chlorine and bromine abundance in MORB: The contrasting behaviour of the Mid-Atlantic Ridge and East Pacific Rise and implications for chlorine geodynamic cycle. Chem. Geol., 126, 101–117.

Jerram, D.A., Martin, V.M., 2008. Understanding crystal populations and their significance through the magma plumbing population. Annen, C. and Zellmer, G.F. (eds) Dyanamics of

Crustal Magma Transfer, Storage and Differentiation. Geol. Soc., London, Special Publications, 304, 133-148. doi: 10.1144/SP304.7

Kamenetsky, V.S., Eggins, S.M., Crawford, A.J., Green, D.H., Gasparon, M., Falloon, T.J., 1998. Calcic melt inclusions in primitive olivine at 43° N MAR: evidence for melt–rock reaction/melting involving clinopyroxene-rich lithologies during MORB generation. Earth Planet. Sci. Lett., 160, 115–132.

Kendrick, M.A., Arculus, R., Burnard, P., Honda, M., 2013. Quantifying brine assimilation by submarine magmas: Examples from the Galapagos Spreading Centre and Lau Basin. Geochim. Cosmochim. Acta, 123, 150–165. doi:10.1016/j.gca.2013.09.012.

Kendrick, M.A., Jackson, M.G., Hauri, E.H., Phillips, D., 2015. The halogen (F, Cl, Br, I) and H_2O systematics of Samoan lavas: assimilated-seawater, EM2 and high-$^3He/^4He$ components. Earth Planet. Sci. Lett., 410, 197-209.

Kent, A.J., Norman, M.D., Hutcheon, I.D., Stolper, E.M., 1999a. Assimilation of seawater-derived components in an oceanic volcano: Evidence from matrix glasses and glass inclusions from Loihi seamount, Hawaii. Chem. Geol., 156, 299–319.

Kent, A.J., Clague, D.A., Honda, M., Stolper, E.M., Hutcheon, I.D., Norman, M.D., 1999b. Widespread assimilation of a seawater-derived component at Loihi Seamount, Hawaii. Geochim. Cosmochim. Acta, 63, 2749–2761.

Koornneef, J.M., Nikogosian, I., van Bergen, M.J., Smeets, R., Bouman, C., Davies, G.R., 2015. TIMS analysis of Sr and Nd isotopes in melt inclusions from Italian potassium-rich lavas using prototype 10^{13} Ω amplifiers. Chem. Geol. 397, 14-23.

Koppers, A.A.P., Russell, J.A., Jackson, M.G., Konter, J., Staudigel, H., Hart, S.R., 2008. Samoa reinstated as a primary hotspot trail. Geology, 36, 435–438. doi:10.1130/G24630A.1.

Koppers, A. A. P., Russell, J.A., Roberts, J., Jackson, M.G., Konter, J., Wright, D.J., Staudigel, H., Hart, S.R., 2011. Age systematics of two young en echelon Samoan volcanic trails. Geochem. Geophys. Geosyst. 12, Q07025. doi:10.1029/2010GC003438.

Kurz, M.D., Jenkins, W.J., Hart, S.R., 1982. Helium isotopic systematics of oceanic islands and mantle heterogeneity. Nature, 297, 43–47.

Kurz, M.D., Geist, D., 1999. Dynamics and evolution of the Galapagos hotspot from helium isotope geochemistry. Geochim. Cosmochim. Acta, 63, 4139-4156

Kurz, M.D., Curtice, J.C., Lott III, D.E., Solow, A., 2004. Rapid helium isotopic variability in Mauna Kea shield lavas from the Hawaiian Scientific Drilling Project. Geochem. Geophys. Geosyst. 4, Q04G14. doi:10.1029/2002GC000439.

Lassiter, J.C., Hauri, E.H., Nikogosian, I.K., Barsczus, H.G., 2002. Chlorine–potassium variations in melt inclusions from Raivavae and Rapa, Austral Islands: Constraints on chlorine recycling in the mantle and evidence for brine-induced melting of oceanic crust. Earth Planet. Sci. Lett., 202, 525–540.

Maclennan, J., 2008. Lead isotope variability in olivine-hosted melt inclusions from Iceland, Geochim. Cosmochim. Acta 72, 4159–4176.

McDougall, I., 2010. Age of volcanism and its migration in the Samoa Islands, Geol. Mag., 147(5), 705–717

Michael, P.J., Schilling, J.G., 1989. Chlorine in mid-ocean ridge magmas: Evidence for assimilation of seawater-influenced components. Geochim. Cosmochim. Acta, 53, 3131–3143.

Mokadem F., Parkinson, I.J., Hathorne, E.C., Anand, P., Allen, J.T., Burton, K.W., 2015. High-precision radiogenic strontium isotope measurements of the modern and glacial ocean: limits on glacial–interglacial variations in continental weathering. Earth Planet. Sci. Lett. 415, 111–120.

Parman, S.W., Kurz, M.D., Hart, S.R., Grove, T.L., 2005. Helium solubility in olivine and implications for high $^{3}He/^{4}He$ in ocean island basalts. Nature 437, 1140–1143.

Ramos, F.C., Reid, M.R., 2005. Distinguishing melting of heterogeneous mantle sources from crustal contamination: insights from Sr isotopes at the Phenocryst Scale, Pisgah Crater, California J. Petrol. 46:999–1012.

Remmert P., Dohmen R., Chakraborty S., 2008. Diffusion of REE, Hf and Sr in olivine. Eos Trans. AGU, 89(53) Fall Meet. Suppl. MR33A-1844 (abstr.)

Roeder, P.L., Emslie, R.F. , 1970. Olivine–liquid equilibrium. Contribution to Mineralogy and Petrology 29, 275–289.

Saal, A.E., Hart, S.R., Shimizu, N., Hauri, E.H., Layne, G.D., 1998. Pb isotopic variability in melt inclusions from oceanic island basalts, Polynesia. Science 282:1481-1484.

Saal, A.E., Hart, S.R., Shimizu, N., Hauri, E.H., Layne, G.D., Eiler, J.M., 2005. Pb isotopic variability in melt inclusions from the EMI-EMII-HIMU mantle end-members and the role of oceanic lithosphere. Earth Planet. Sci. Lett. 240:605–20.

Salters, V.J.M., Mallick, S., Hart, S.R., Langmuir, C.E., Stracke, A., 2011. Domains of depleted mantle: New evidence from hafnium and neodymium isotopes. Geochem. Geophys. Geosyst., 12, Q08001, doi:10.1029/2011GC003617.

Sims, K.W.W., Hart, S.R., Reagan, M.K., Blusztajn, J., Staudigel, H., Sohn, R.A., Layne, G.D., Ball, L.A., 2008. ^{238}U-^{230}Th-^{226}Ra-^{210}Pb-^{210}Po, ^{232}Th-^{228}Ra, and ^{235}U-^{231}Pa constraints on the ages and petrogenesis of Vailulu’u and Malumalu Lavas, Samoa. Geochem. Geophys. Geosyst., 9. Q04003, doi:10.1029/2007GC001651.

Sobolev, A.V., Hofmann, A.W., Jochum, K.P., Kuzmin, D.V., Stoll, B., 2011. A young source for the Hawaiian plume. Nature, 476, 434–437.

Stracke, A., Hofmann, A.W., Hart, S.R., 2005. FOZO, HIMU, and the rest of the mantle zoo. Geochem., Geophys., Geosyst., 6. doi:10.1029/2004GC000824.

Staudigel, H., Hart, S.R., Pile, A., Bailey, B.E., Baker, E.T., Brooke, S., Connelly, D.P., Haucke, L., German, C.R., Hudson, I., Jones, D., Koppers, A.A.P., Konter, J., Lee, R., Pietsch, T.W., Tebo, B.M., Templeton, A.S., Zierenberg, R., Young, C.M., 2006. Vailulu'u seamount, Samoa: Life and death on an active submarine volcano. Proc. Nat. Acad. Sci. U.S.A. 103:6448-6453.

Stroncik, N.A., Haase, K.M., 2004. Chlorine in oceanic intraplate basalts: Constraints on mantle sources and recycling processes. Geology 32, 945. doi:10.1130/G21027.1.

Taylor, B., 2006. The single largest oceanic plateau: Ontong Java-Manihiki-Hikurangi, Earth Planet. Sci. Lett., 241, 372–380.

Trull, T.W., Kurz, M.D., Jenkins, W.J., 1991. Diffusion of cosmogenic 3He in olivine and quartz; implications for surface exposure dating. Earth Planet. Sci. Lett. 103, 241–256.

Valbracht, P., Staudacher, T., Malahoff, A., Moreira, M., Allegre, C., 1997. Noble gas systematics of deep rift zone glasses from Loihi Seamount, Hawaii. Earth Planet. Sci. Lett. 150, 399-412.

White, W. M., 1985. Source of oceanic basalts: Radiogenic isotopic evidence, Geology 13, 115–118.

White, W. M., 2010) Oceanic Island Basalts and mantle plumes: The geochemical perspective. Annu. Rev. Earth Planet. Sci. Lett. 38, 133–160.

White, W.M., 2015. Isotopes, DUPAL, LLSVPs, and Anekantavada. Chem. Geol. 419, 10-28.

Widom, E., Farquhar, J., 2003. Oxygen isotope signatures in olivines from Sa˜o Miguel (Azores) basalts: implications for crustal and mantle processes. Chem. Geol. 193, 237–255.

Workman, R.K., Hart, S.R., Jackson, M.G., Regelous, M., Farley, K.A., Blusztajn, J., Kurz, M.D., 2004. Recycled metasomatised lithosphere as the origin of the Enriched Mantle II (EM2) end-member: Evidence from the Samoan Volcanic Chain. Geochem. Geophys. Geosys., 5, doi:10.1029/2003GC000623.

Workman, R.K., Hauri, E., Hart, S.R., Wang, J., Blusztajn, J., 2006. Volatile and trace elements in basaltic glasses from Samoa: Implications for water distribution in the mantle. Earth Planet. Sci. Lett., 241, 932–951.

Workman, R.K., Hart, S.R., Eiler, J.M., Jackson, M.G., 2008. Oxygen isotopes in Samoan lavas: confirmation of continent recycling. Geology, 36, 551-554.

Wright, E., White, W.M., 1987. The origin of Samoa: New evidence from Sr, Nd, and Pb isotopes, Earth Planet. Sci. Lett., **81**, 151–162, doi:10.1016/0012-821X(87)90152-X.

Zindler, A., Hart, S.R., 1986. Chemical geodynamics. Annu. Rev. Earth Planet. Sci., 14, 493–571.

Table 1. Olivine $^{87}Sr/^{86}Sr$ and Sr concentrations for Samoan samples examined in this study.

Sample	Olivine color	Volcano	Olivine mass (g)	Total Sr (ng)	Olivine Sr conc. (ppm)	Sr blank (ng)	Sample/Blank	$^{87}Sr/^{86}Sr$ olivines[1]	2 σ (std. err)	$^{87}Sr/^{86}Sr$ whole rock[2]	$\Delta\ ^{87}Sr/^{86}Sr_{wr\text{-}oliv}$	Cl/K [3]	$^3He/^4He$ [4]	$\delta^{18}O$ [5]
T25		Ta'u	0.069	31.9	0.461	0.019	1661	0.704647	0.000008	0.704708	87		13.3	5.3
T-25 rep 1		Ta'u	0.094	34.4	0.364	0.047	735	0.704652	0.000009	0.704708	79			
T-25 rep 2		Ta'u	0.092	38.3	0.417	0.047	819	0.704653	0.000009	0.704708	78			
T-25 rep 3		Ta'u	0.092	44.0	0.476	0.047	942	0.704662	0.000005	0.704708	65			
T33		Ta'u	0.073	18.0	0.248	0.019	935	0.704777	0.000025	0.704736	-58		16.6	5.24
OFU 04-03		Ofu	0.095	55.8	0.590	0.019	2905	0.704722	0.000012	0.704756	49		24.0	
ALIA-104-04		Muli	0.068	14.4	0.212	0.031	459	0.704823	0.000021	0.704831	11	0.176	18.6	
AVON3-63-2	brown	Vailulu'u	0.097	25.9	0.266	0.031	825	0.705516	0.000015	0.705385	-185		10.1	5.34
AVON3-63-11	brown	Vailulu'u	0.185	100.6	0.543	0.053	1914	0.705467	0.000017	0.705394	-103		10.2	5.35
AVON3-73-2		Vailulu'u	0.096	59.9	0.622	0.019	3120	0.705294	0.000008	0.705424	184		9.3	5.11
AVON3-68-11	brown	Vailulu'u	0.091	18.0	0.198	0.038	481	0.705249	0.000013	0.705594	489			
AVON3-68-11	green	Vailulu'u	0.099	16.0	0.161	0.038	427	0.705433	0.000014	0.705594	229			
AVON3-71-2	brown	Vailulu'u	0.174	68.5	0.393	0.053	1304	0.705436	0.000013	0.705943	718	0.169	9.5	5.42
AVON3-71-2	green	Vailulu'u	0.153	61.8	0.404	0.025	2487	0.705404	0.000015	0.705943	763		9.5	5.42
AVON3-78-1		Malumalu	0.077	19.9	0.258	0.031	633	0.707521	0.000032	0.708901	1947	0.042	8.1	5.53
AVON3-78-1 Leeds Rep [6]		Malumalu	0.077	38.3	0.496	0.070	547	0.707773	0.000070	0.708901	1591			
AVON3-78-1 VU Rep [6]		Malumalu	0.019	13.0	0.667	0.028	464	0.707385	0.000009	0.708901	2139			

1. Following spike deconvolution and correction for mass bias, all data are corrected for the offset between the accepted (0.710240) and measured $^{87}Sr/^{86}Sr$ of NBS987 runs made on the same date of analysis. $^{87}Sr/^{86}Sr$ ratios are also corrected for blank.
2. Whole rock $^{87}Sr/^{86}Sr$ data are from Workman et al. (2004, 2008) and Jackson et al. (2007, 2010, 2011, 2014).
3. Cl/K data are measured on submarine pillow glasses, and are from Workman et al. (2006) and Kendrick et al. (2015). Only 3 samples examined in this study have associated submarine glass that can be used for Cl/K analysis.
4. $^3He/^4He$ data are from the following sources: Workman et al. (2004), Jackson et al. (2007), Jackson et al. (2010, 2014).
5. All $\delta^{18}O$ measurements were made on olivines, and are published in Workman et al. (2008).
6. Replicate analyses on a different subset of olivines from AVON3-78-1 underwent separate leaching, chemical separation and mass spectrometery at VU and University of Leeds.

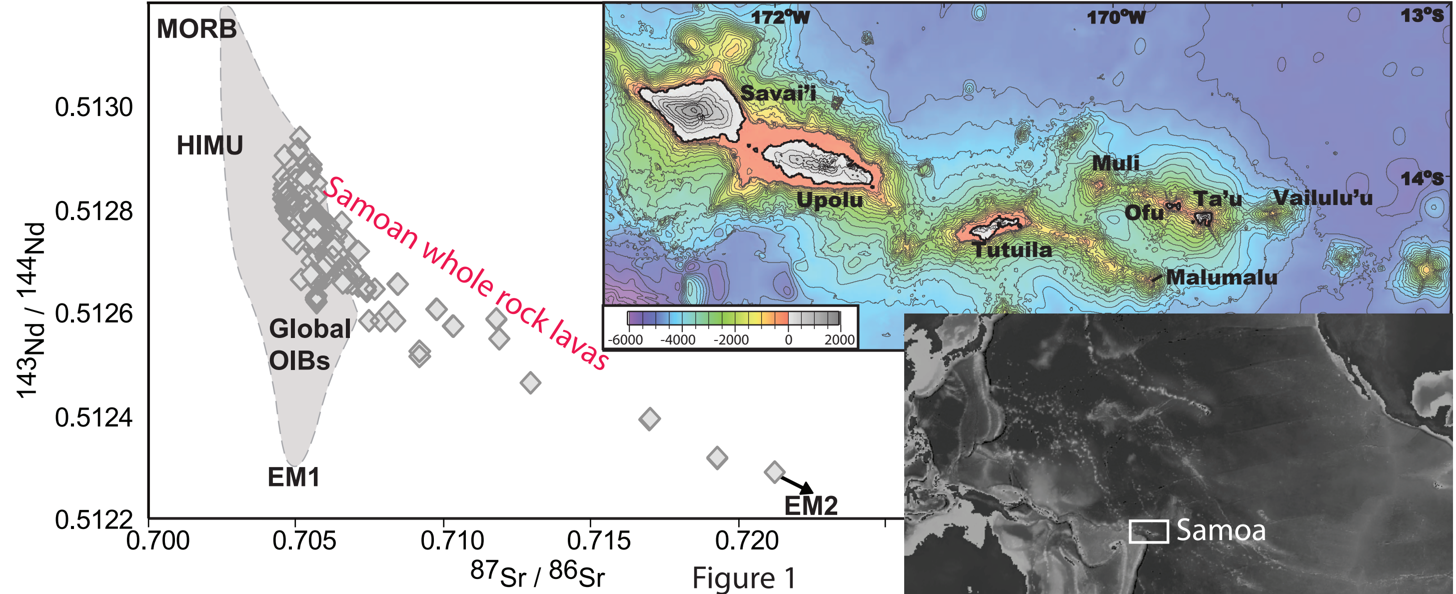
MORB
HIMU
Global
OIBs
EM1
EM2
Samoan whole rock lavas
0.5130
0.5128
0.5126
0.5124
0.5122
143Nd / 144Nd
0.700
0.705
0.710
0.715
0.720
87Sr / 86Sr
172°W
170°W
13°S
14°S
Savai'i
Upolu
Tutuila
Muli
Ofu
Ta'u
Vailulu'u
Malumalu
-6000
-4000
-2000
0
2000
Samoa
Figure 1

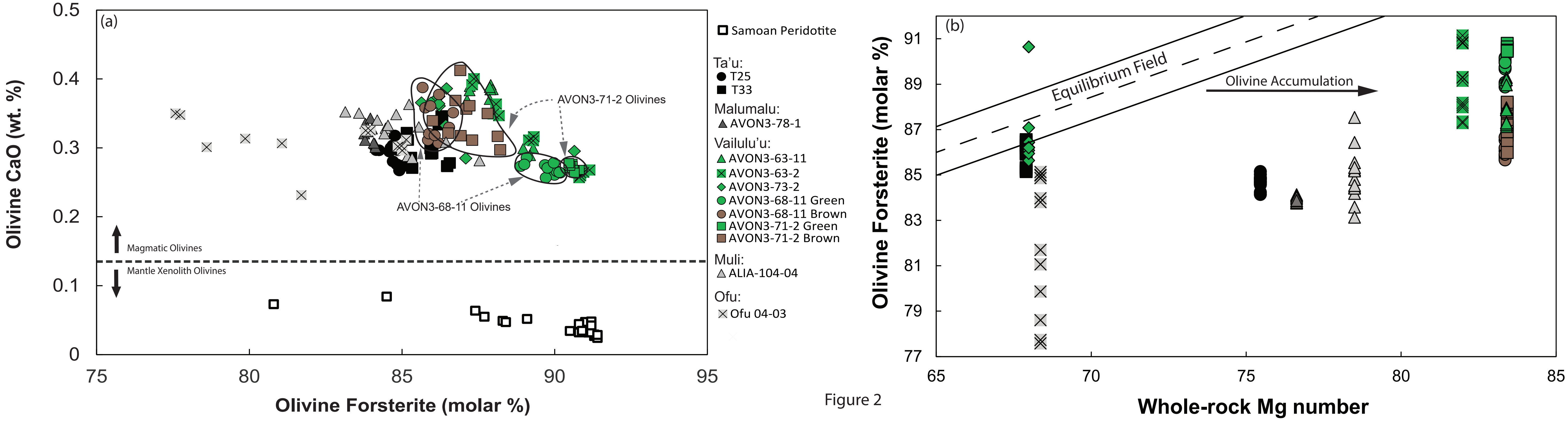

(a)
Olivine CaO (wt. %)
Olivine Forsterite (molar %)
0.5
0.4
0.3
0.2
0.1
0
75
80
85
90
95
AVON3-71-2 Olivines
AVON3-68-11 Olivines
Magmatic Olivines
Mantle Xenolith Olivines
Samoan Peridotite
Ta'u:
T25
T33
Malumalu:
AVON3-78-1
Vailulu'u:
AVON3-63-11
AVON3-63-2
AVON3-73-2
AVON3-68-11 Green
AVON3-68-11 Brown
AVON3-71-2 Green
AVON3-71-2 Brown
Muli:
ALIA-104-04
Ofu:
Ofu 04-03
(b)
Olivine Forsterite (molar %)
Whole-rock Mg number
91
89
87
85
83
81
79
77
65
70
75
80
85
Equilibrium Field
Olivine Accumulation

Figure 2

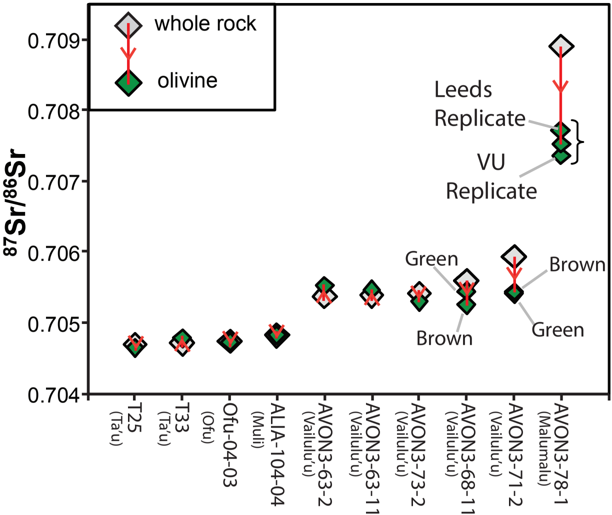

whole rock
olivine
Leeds
Replicate
VU
Replicate
Green
Brown
Brown
Green
87Sr/86Sr
0.709
0.708
0.707
0.706
0.705
0.704
T25
(Ta'u)
T33
(Ta'u)
Ofu-04-03
(Ofu)
ALIA-104-04
(Muli)
AVON3-63-2
(Vailulu'u)
AVON3-63-11
(Vailulu'u)
AVON3-73-2
(Vailulu'u)
AVON3-68-11
(Vailulu'u)
AVON3-71-2
(Vailulu'u)
AVON3-78-1
(Malumalu)

Fig. 3

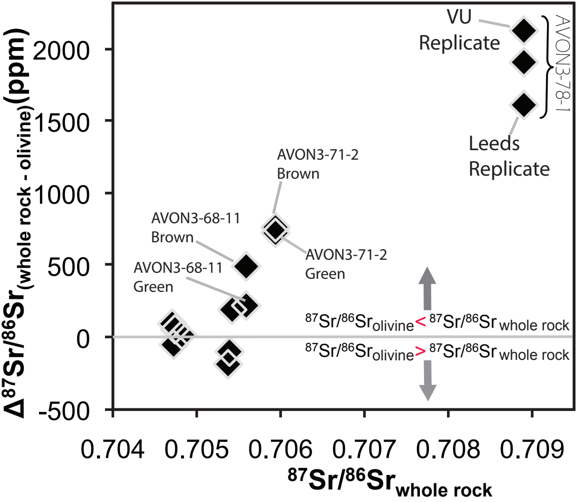

VU
Replicate
AVON3-78-1
Leeds
Replicate
AVON3-71-2
Brown
AVON3-68-11
Brown
AVON3-71-2
Green
AVON3-68-11
Green
87Sr/86Sr olivine < 87Sr/86Sr whole rock
87Sr/86Sr olivine > 87Sr/86Sr whole rock
Δ87Sr/86Sr(whole rock - olivine)(ppm)
2000
1500
1000
500
0
-500
0.704
0.705
0.706
0.707
0.708
0.709
87Sr/86Sr whole rock

Fig. 4

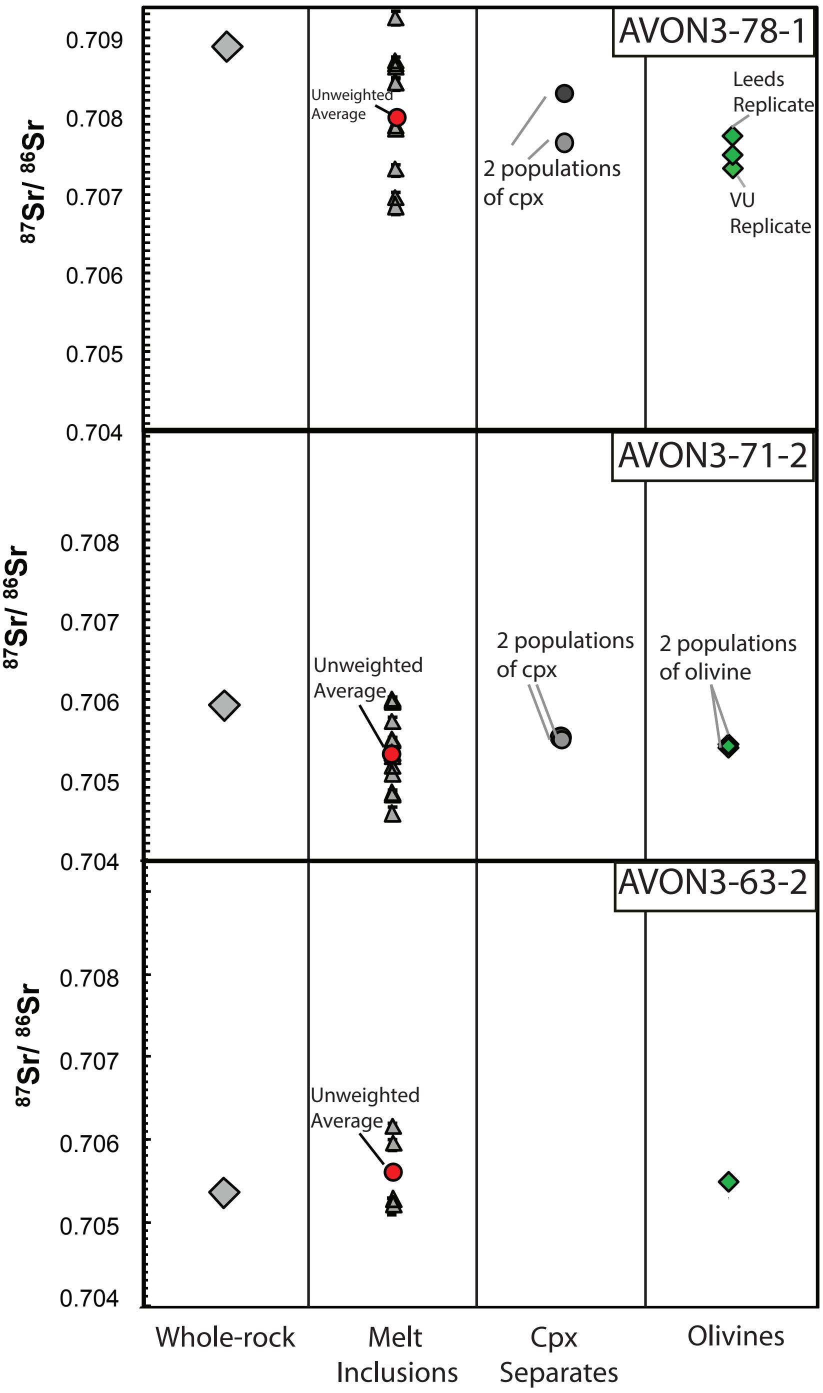
AVON3-78-1
AVON3-71-2
AVON3-63-2
$^{87}Sr/^{86}Sr$
0.709
0.708
0.707
0.706
0.705
0.704
Unweighted Average
2 populations of cpx
Leeds Replicate
VU Replicate
2 populations of olivine
Whole-rock
Melt Inclusions
Cpx Separates
Olivines

Figure 5

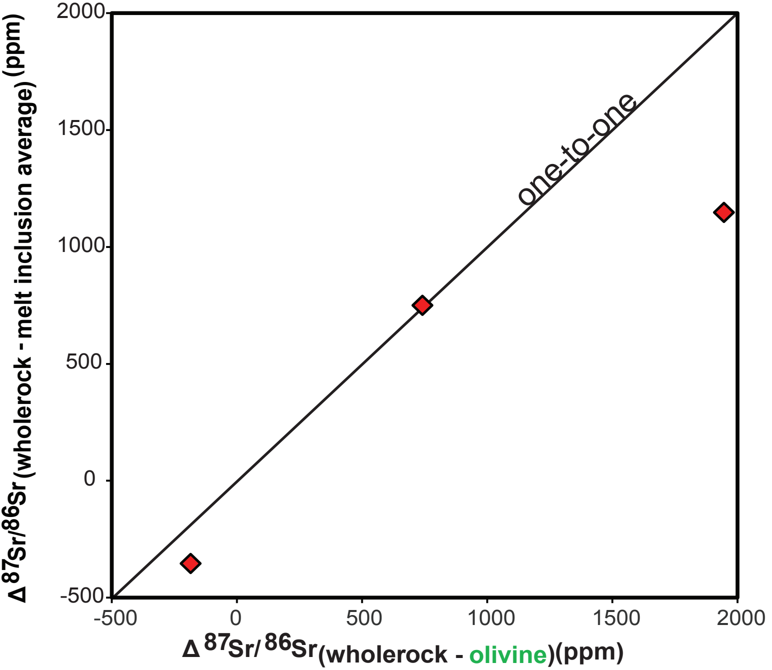
2000
1500
1000
500
0
-500
-500
0
500
1000
1500
2000
one-to-one
Δ 87Sr/86Sr (wholerock - melt inclusion average) (ppm)
Δ 87Sr/ 86Sr (wholerock - olivine)(ppm)

Figure 6

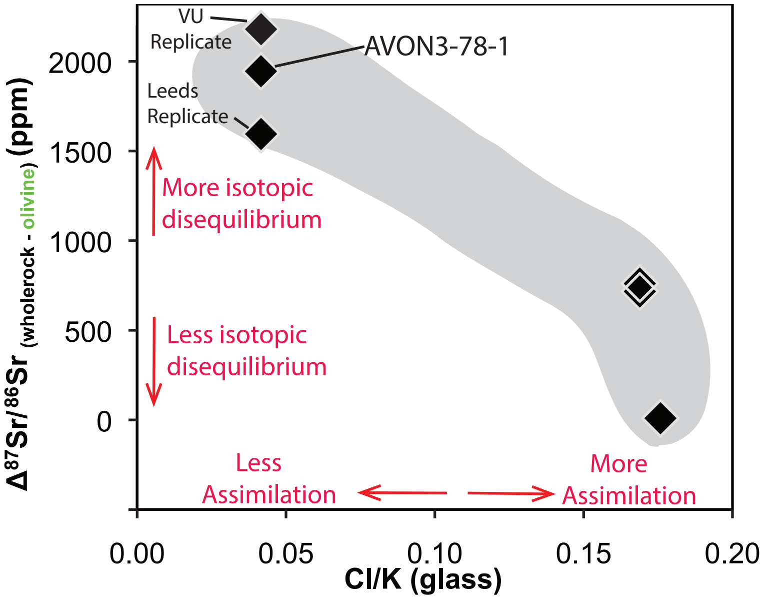
VU
Replicate
AVON3-78-1
Leeds
Replicate
More isotopic
disequilibrium
Less isotopic
disequilibrium
Less
Assimilation
More
Assimilation
2000
1500
1000
500
0
0.00
0.05
0.10
0.15
0.20
Cl/K (glass)
Δ87Sr/86Sr (wholerock - olivine) (ppm)

Figure 7.

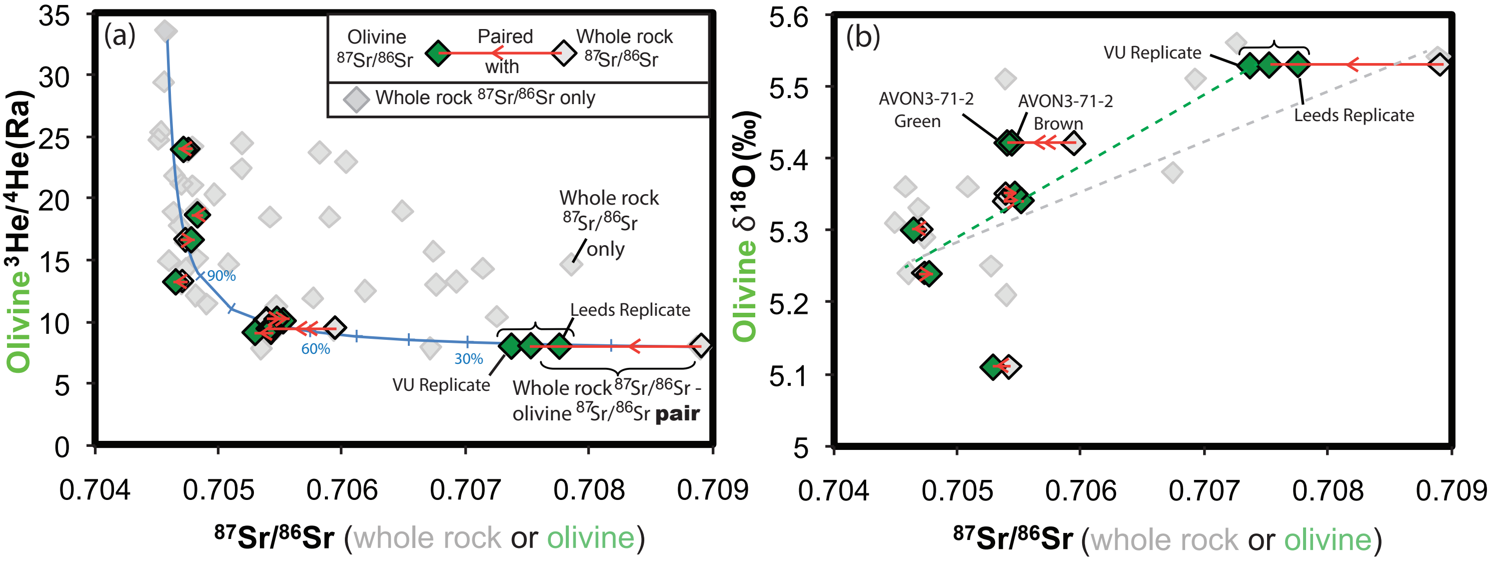
(a)
Olivine 87Sr/86Sr
Paired with
Whole rock 87Sr/86Sr
Whole rock 87Sr/86Sr only
Whole rock 87Sr/86Sr only
90%
60%
30%
Leeds Replicate
VU Replicate
Whole rock 87Sr/86Sr - olivine 87Sr/86Sr pair
Olivine 3He/4He(Ra)
87Sr/86Sr (whole rock or olivine)
(b)
VU Replicate
Leeds Replicate
AVON3-71-2 Green
AVON3-71-2 Brown
Olivine δ18O(‰)
87Sr/86Sr (whole rock or olivine)

Figure 8.

Supplementary Material

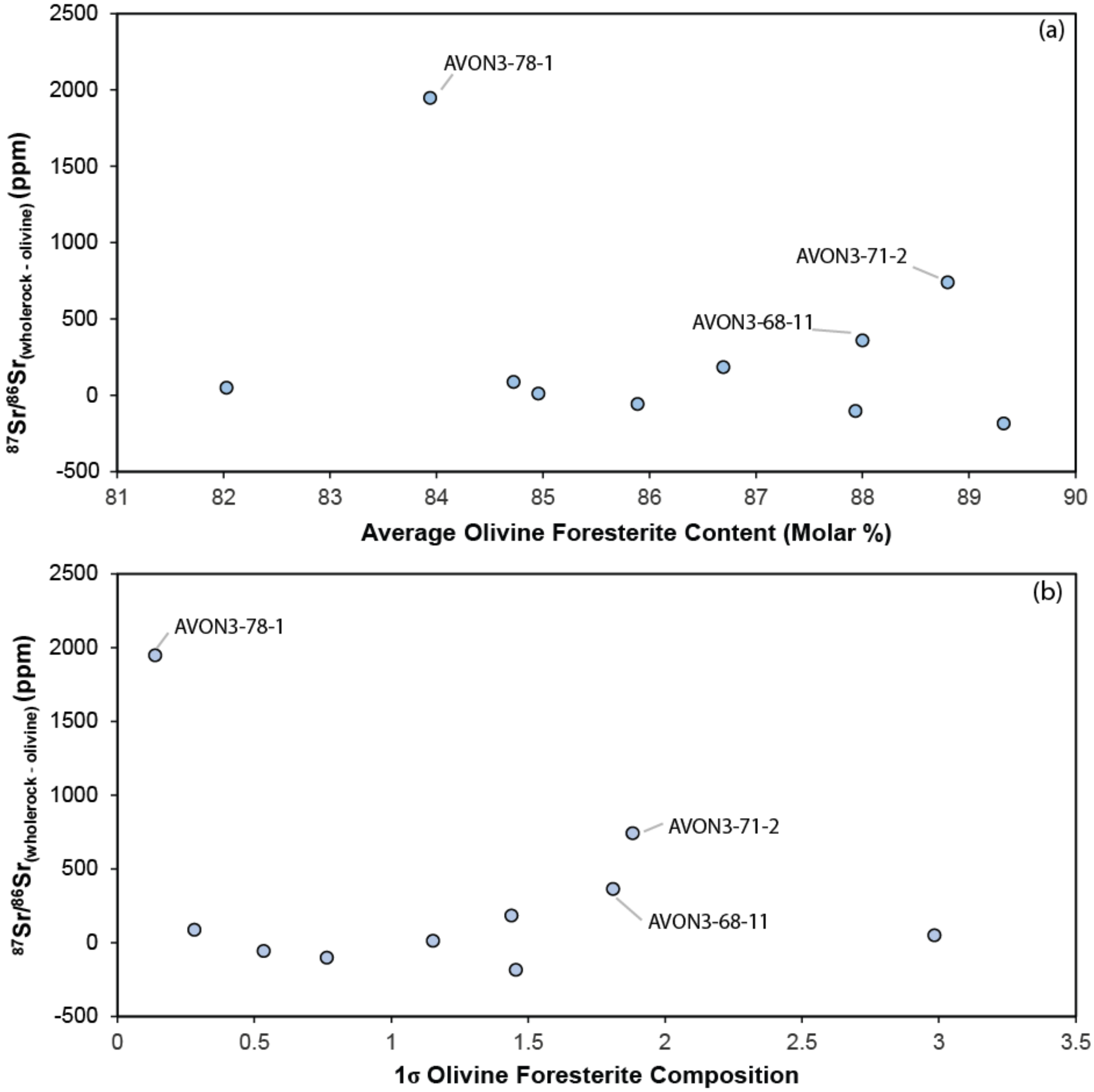

Supplementary Figure 1. (a) $\Delta\,^{87}Sr/^{86}Sr$ whole rock-olivine is compared with average olivine forsterite compositions and variability in forsterite compositions in each sample. (b) The forsterite compositional variability is described using the 1 σ standard deviation of forsterite values for olivines in each basalt (see Supplementary Table 3). For samples AVON3-71-2 and AVON3-68-11, where two populations of olivines were separated (green and brown), the variability in olivine compositions (1σ) and average forsterite contents were calculated for the entire olivine population of the lava (i.e. the green and brown populations are combined). Additionally, where two populations of olivines were separated the average whole rock- olivine $^{87}Sr/^{86}Sr$ disequilibrium for the populations is used.

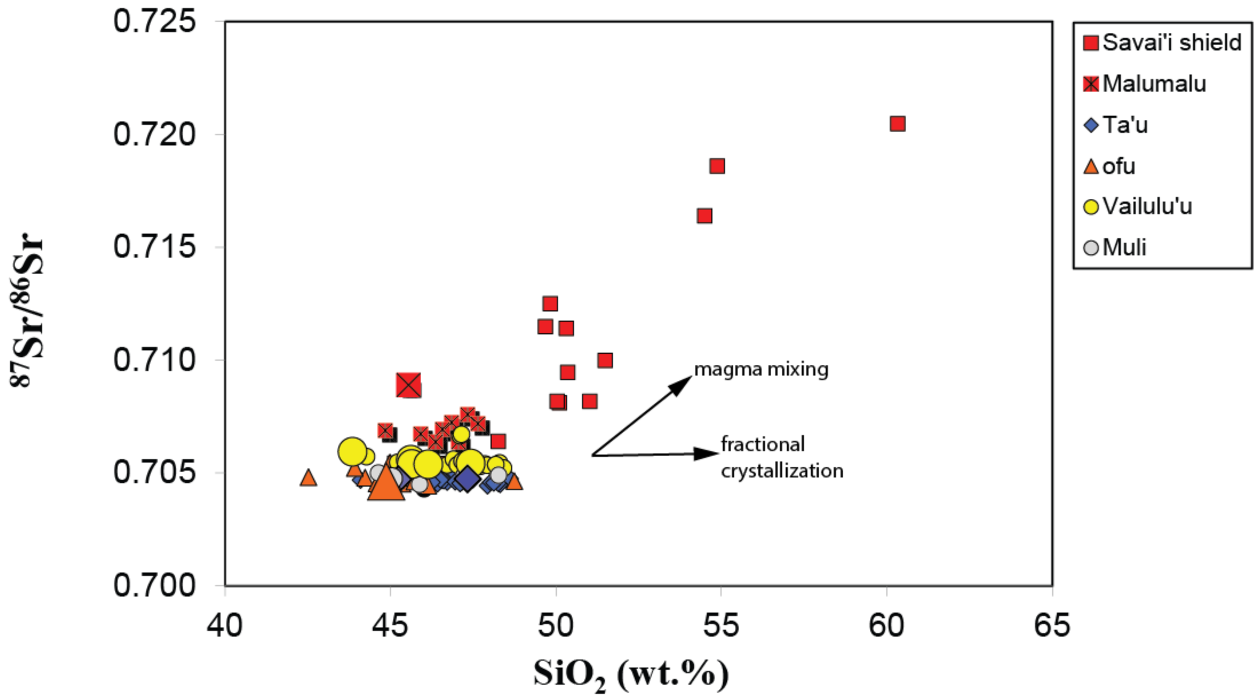

Supplementary Figure 2. Whole rock $^{87}Sr/^{86}Sr$ and SiO_2 data are compared for all lavas from the 5 volcanoes (Ta'u, Malumalu, Ofu, Muli and Vailulu'u) from which the samples examined in this study were collected. Additionally, all available fresh shield lavas from Savai'i (from dredges 114, 115 and 128 in Jackson et al., 2007) are shown to illustrate the observation that high $^{87}Sr/^{86}Sr$ lavas have high SiO_2. These high $^{87}Sr/^{86}Sr$, high SiO_2 lavas host little to no olivine. Major element data are not corrected for fractionation. There are lavas from other Samoan volcanoes that have low $^{87}Sr/^{86}Sr$ and high SiO_2 (e.g., Tutuila) that fall of the trend show in this figure, but lavas from these volcanoes were not examined in this study. The larger symbols represent the samples examined in this study. The whole rock major element data for samples examined in this study are available in supplementary table 2. Whole rock major element and $^{87}Sr/^{86}Sr$ data used in this plot are from Workman et al. (2004), Jackson et al. (2007, 2010) and Hart and Jackson (2014).

Supplementary References

Hart, S. R., Jackson, M.G. (2014). Ta'u and Ofu/Olosega volcanoes: The ''twin sisters'' of Samoa, their P, T, X melting regime, and global implications, Geochem. Geophys. Geosyst 15, 2301–2318

Jackson, M.G., Hart, S.R., Koppers, A.A.P., Staudigel, H., Konter, J., Blusztajn, J., Kurz, M.D., Russell, J.A. (2007a). The return of subducted continental crust in Samoan lavas. Nature, 448, 684-687.

Jackson, M.G., Hart, S.R., Konter, J.P., Koppers, A.A.P., Staudigel, H., Kurz, M.D., Blusztajn, J., Sinton, J.M., (2010), The Samoan hotspot track on a "hotspot highway": Implications for mantle plumes and a deep Samoan mantle source. Geochem. Geophys. Geosyst. doi:10.1029/2010GC003232

Workman, R.K., Hart, S.R., Jackson, M.G., Regelous, M., Farley, K.A., Blusztajn, J., Kurz, M.D. (2004). Recycled metasomatised lithosphere as the origin of the Enriched Mantle II (EM2) end-member: Evidence from the Samoan Volcanic Chain. Geochem. Geophys. Geosys., 5, doi:10.1029/2003GC000623.